Raman optical activity (ROA) and conformational flexibility of (bio)molecules in solution

Vladimír Baumruk

Charles University in Prague
Faculty of Mathematics and Physics
Institute of Physics

Vibrational Spectroscopy

- infrared spectroscopy (IR)
- Raman spectroscopy (RS)

Vibrational Optical Activity (VOA)

- Vibrational Circular Dichroism (VCD)
- Raman Optical Activity (ROA)

Raman Optical Activity - principles

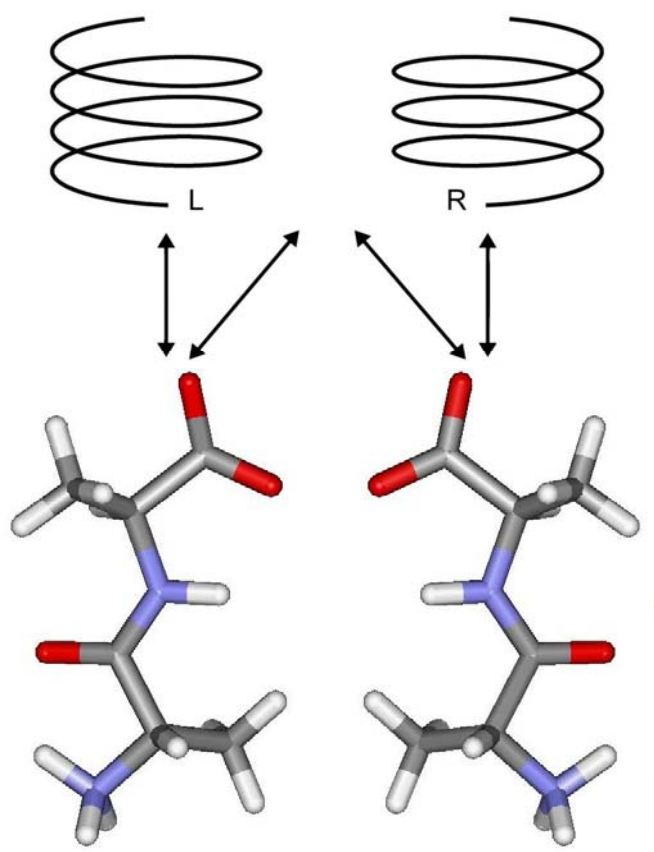

L-alanyl-L-alanine D-alanyl-D-alanine

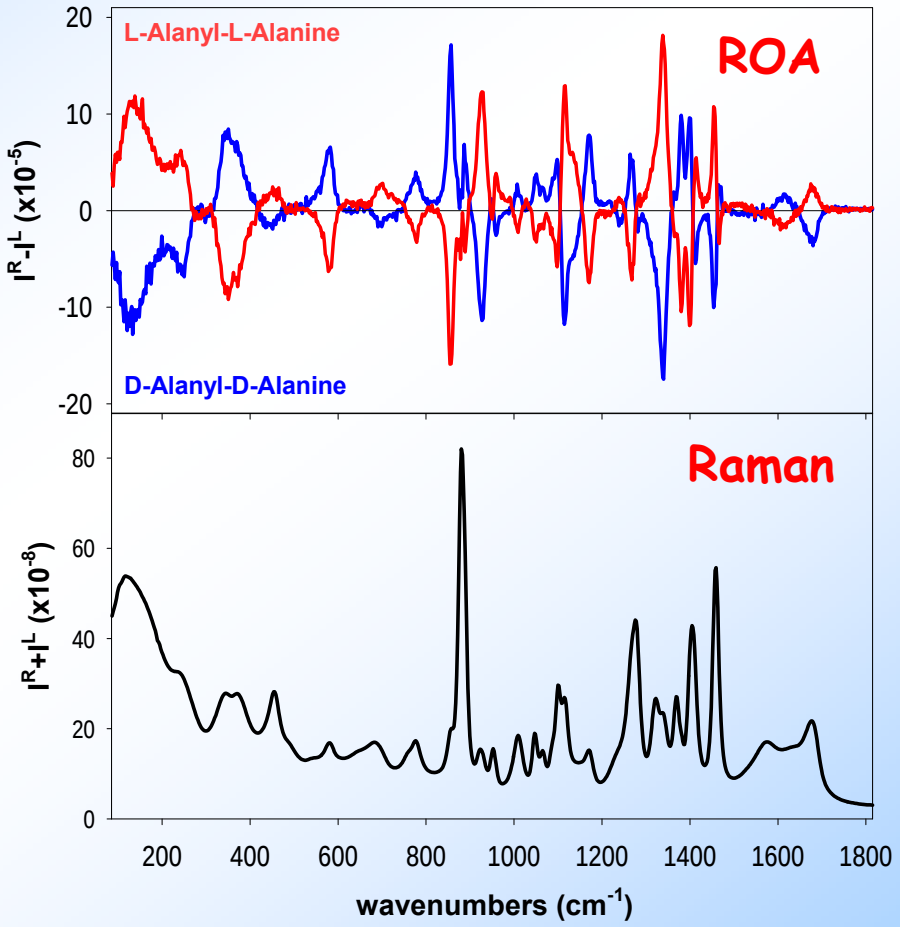

The sensitivity of optical activity to mirror-symmetry properties of chiral molecules is the source of its remarkable ability to specify absolute stereochemical properties of chiral molecules in solution.

Raman optical activity (ROA)

- method of vibrational optical activity (VOA); complementary to vibrational circular dichroism (VCD) in a similar way like Raman spectroscopy is complementary to IR spectroscopy,
- difference technique – difference in response of a *chiral molecule* with respect to *right and left circularly polarized light,*
- combines the *stereochemical sensitivity* of natural optical activity with the *rich structural content* and *conformational sensitivity* of vibrational spectroscopy,
- the time scale of the Raman scattering event (~ 10^{-14} s), is much shorter than that of the fastest conformational fluctuations in biomolecules ⇒ the *ROA spectrum is a superposition of 'snapshot' spectra from all the distinct chiral conformers present in the sample* ⇒ *enhanced sensitivity to the dynamic aspects of biomolecular structure.*

Vibrational optical activity

The sign and magnitude of VCD are conveniently expressed as the dimensionless *anisotropy ratio* defined as a ratio of the experimental VCD band absorbance to the experimental IR band absorbance

$$g \equiv \Delta\varepsilon/\varepsilon = \left(\varepsilon_L - \varepsilon_R\right) \Big/ \left(\varepsilon_L + \varepsilon_R\right) \qquad g = \frac{4R}{D} = \frac{4\,\mathrm{Im}\left(\vec{\mu}.\vec{m}\right)}{\left|\vec{\mu}\right|^2}$$

ROA intensity is usually expressed as dimensionless ratio known as the *circular intensity difference*

$$\Delta \equiv \left(I_R - I_L\right) \Big/ \left(I_R + I_L\right)$$

Anisotropy ratio $\Delta\varepsilon/\varepsilon$ and circular intensity difference Δ are proportional to d/λ (d is a typical internuclear distance in a molecule and λ is the wavelength of the light)

- in the near UV region $\Delta\varepsilon/\varepsilon$ is typically 10^{-3} (ECD),
- in the IR region $\Delta\varepsilon/\varepsilon$ is typically $10^{-4} \div 10^{-5}$ (VCD),
- in the visible region Δ is typically $10^{-3} \div 10^{-4}$ (ROA).

Raman optical activity – experimental geometry

Raman scattering and therefore ROA is associated with a two-photon process

⇒ in comparison to VCD, ROA is inherently more complex, both theoretically and experimentally.

⇒ there are many distinct forms of ROA from which to chose in setting up an experiment

- the scattering geometry (scattering angle),
- modulation scheme.

Scattering angle ξ can generally have any value between 0° and 180° but ROA is usually measured in

- backscattering geometry (ξ =180°),
- right-angle scattering geometry (ξ =90°),
- forward scattering geometry (ξ =0°).

Raman optical activity – modulation schemes

- incident circular polarization (ICP)
- scattered circular polarization (SCP)
- in-phase dual circular polarization (DCPI)
- out-of-phase dual circular polarization (DCPII)

If one seeks the **optimum ROA intensity** for a given investment in incident laser intensity, the **backscattering ICP** and **DCPI ROA** have been found to be superior to other approaches.

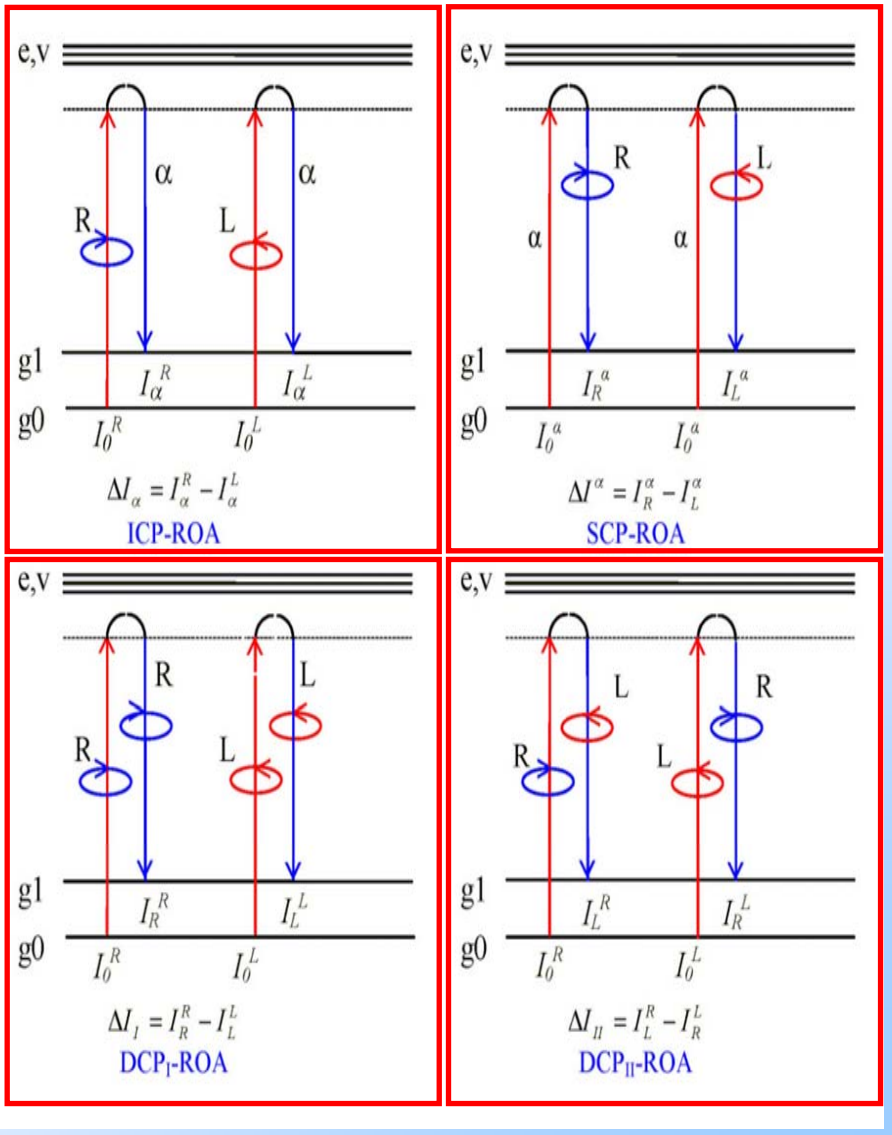

ChiralRAMAN™ – commercial ROA spectrometer from BioTools (SCP)

Prague ROA Spectrometer

- ICP modulation scheme
- backscattering geometry

Block diagram of the spectrometer

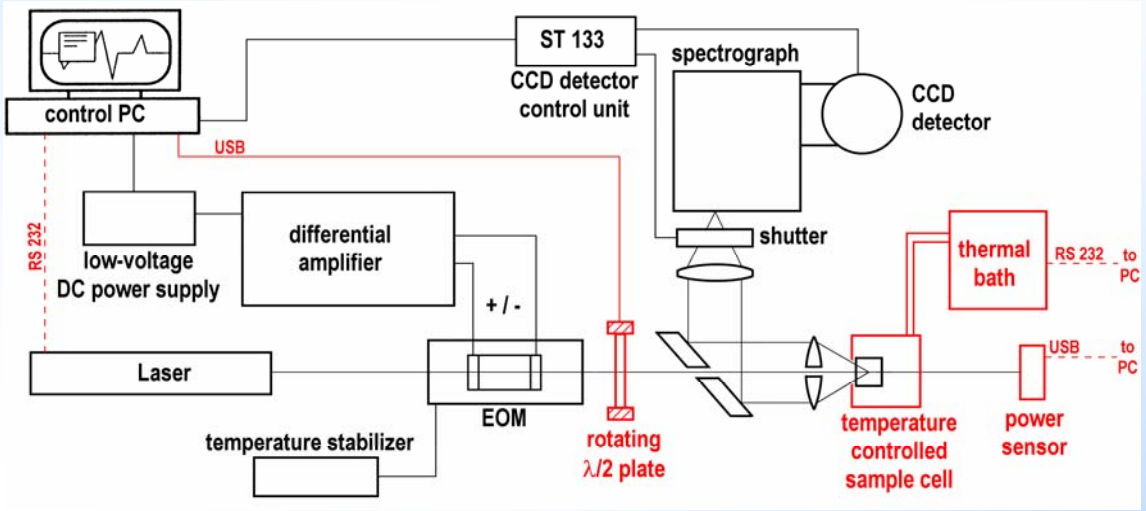

Optical diagram

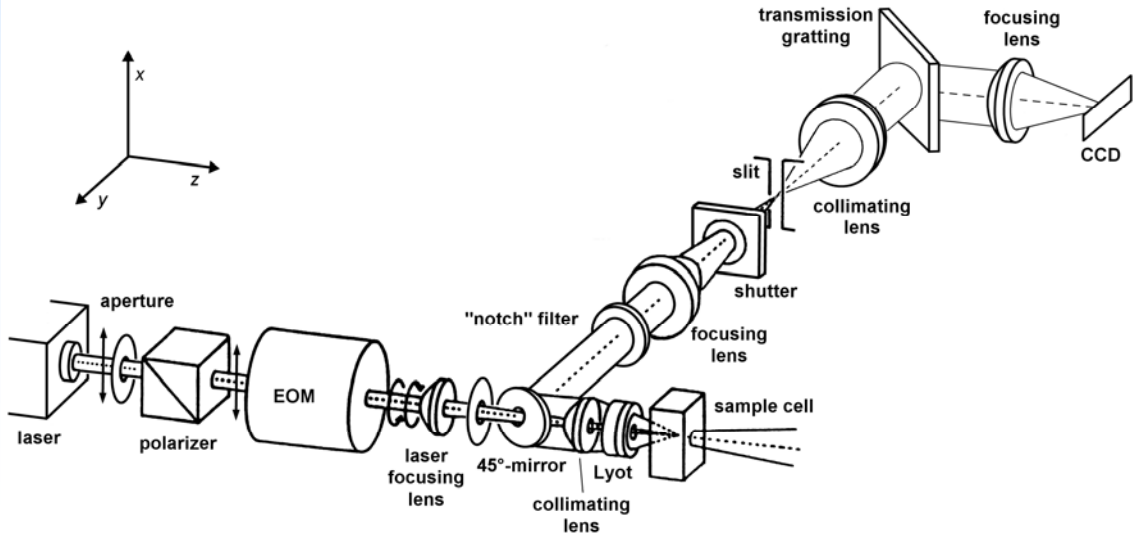

- spectrograph HoloSpec (optical speed **f/1.4**)
- back-illuminated CCD detector 1340x100 pixels
- precise alignment of optical elements

Prague ROA spectrometer

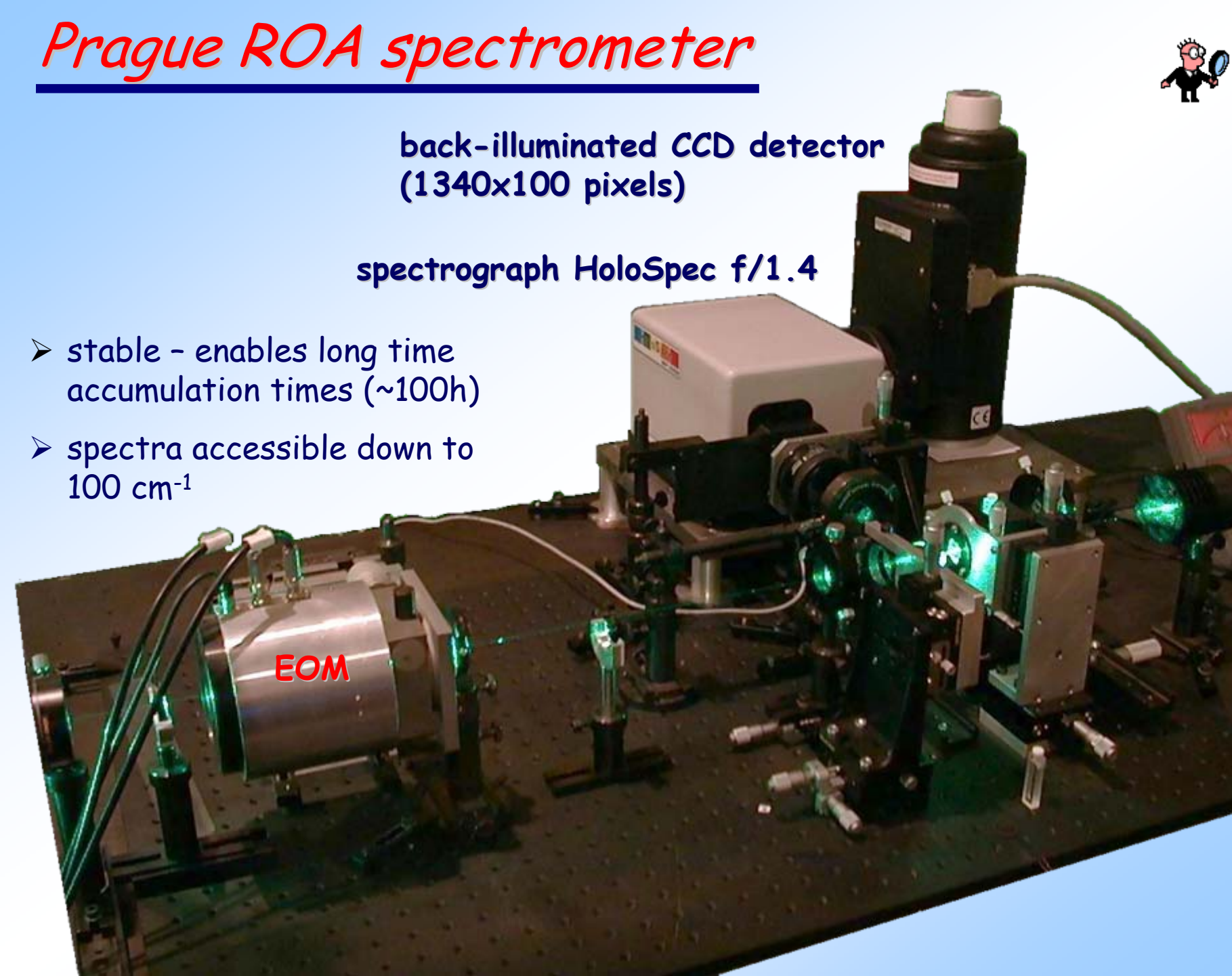

- stable – enables long time accumulation times (~100h)
- spectra accessible down to 100 cm^{-1}

Spectral data treatment

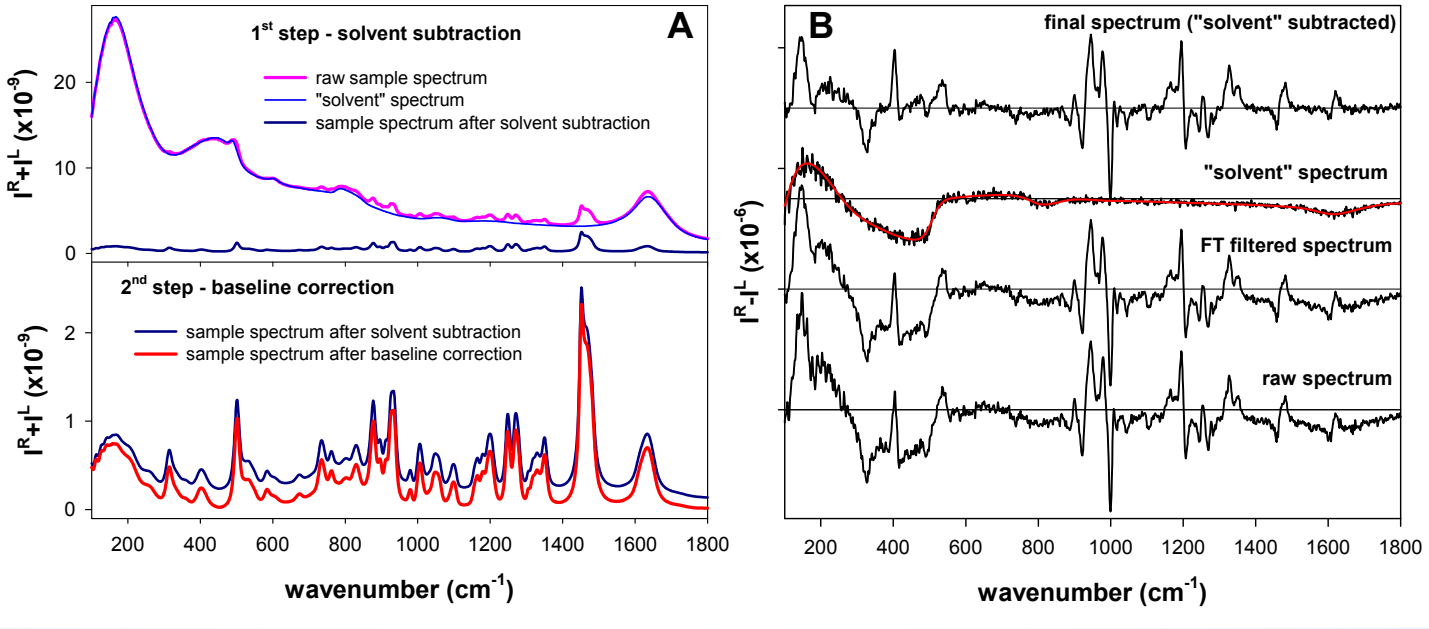

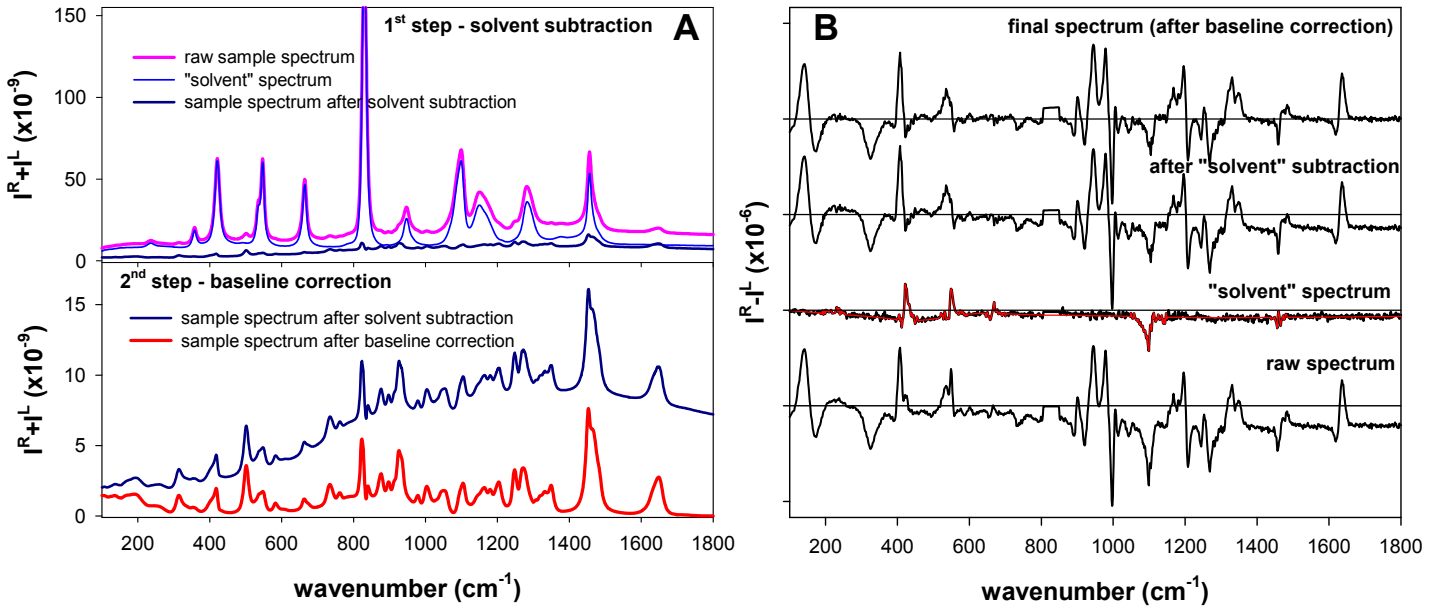

Raman optical activity – basic theory

Raman scattering and ROA – two-photon phenomena ⇒ tensor quantities

ROA – depends on the interaction of molecules with radiation beyond the electric-dipole approximation. In the case of ROA it is both magnetic-dipole and electric-quadrupole interaction (whereas for VCD it is only the magnetic-dipole interaction) .

General ROA theory is complicated, there are two useful approximations:

- far from resonance (FFR)
- strong resonance with a single electronic state (SES)

Raman and ROA intensities can be expressed as a linear combination of invariants of polarizability tensor $\alpha_{\alpha\beta}$ (Raman) a ROA tensors (magnetic dipole $G'_{\alpha\beta}$ and electric quadrupole $A_{\alpha\beta\gamma}$)

- Raman scattering – in the general case 3 invariants, in the FFR only 2
- ROA – in the general case 10 invariants, in the FFR the number of invariants reduces to 3 or to even 2 in case of backscattering geometry

Raman optical activity – basic theory

In the far from resonance approximation:

polarizability tensor

$$\alpha_{\alpha\beta} = \frac{2}{\hbar}\sum_{j\neq n}\left(\frac{\omega_{jn}}{\omega_{jn}^2-\omega^2}\right)\mathrm{Re}\left(\langle n|\mu_\alpha|j\rangle\langle j|\mu_\beta|n\rangle\right)$$

electric dipole-magnetic dipole optical activity tensor

$$G'_{\alpha\beta} = \frac{2}{\hbar}\sum_{j\neq n}\left(\frac{\omega}{\omega_{jn}^2-\omega^2}\right)\mathrm{Im}\left(\langle n|\mu_\alpha|j\rangle\langle j|m_\beta|n\rangle\right)$$

electric dipole-electric quadrupole optical activity tensor

$$A_{\alpha\beta\gamma} = \frac{2}{\hbar}\sum_{j\neq n}\left(\frac{\omega_{jn}}{\omega_{jn}^2-\omega^2}\right)\mathrm{Re}\left(\langle n|\mu_\alpha|j\rangle\langle j|\Theta_{\beta\gamma}|n\rangle\right)$$

isotropic invariants of the polarizability tensor and electric dipole-magnetic dipole optical activity tensor

$$\alpha = \frac{1}{3}\alpha_{\alpha\alpha} \qquad G' = \frac{1}{3}G'_{\alpha\alpha}$$

anisotropic invariants of the

- polarizability-polarizability tensor

$$\beta(\alpha)^2 = \frac{1}{2}\left(3\alpha_{\alpha\beta}\alpha_{\alpha\beta} - \alpha_{\alpha\alpha}\alpha_{\beta\beta}\right)$$

- polarizability-magnetic dipole OA tensor

$$\beta\left(G'\right)^2 = \frac{1}{2}\left(3\alpha_{\alpha\beta}G'_{\alpha\beta} - \alpha_{\alpha\alpha}G'_{\beta\beta}\right)$$

- polarizability-electric quadrupole OA tensor

$$\beta\left(A\right)^2 = \frac{1}{2}\omega\alpha_{\alpha\beta}\varepsilon_{\alpha\gamma\delta}A_{\gamma\delta\beta}$$

Raman optical activity

- circular intensity difference for unpolarized ICP ROA in backscattering geometry

$$\Delta_u\left(180^\circ\right) \equiv \frac{\Delta I_u\left(180^\circ\right)}{I_u\left(180^\circ\right)} = \frac{I_u^R - I_u^L}{I_u^R + I_u^L} = \frac{\frac{48}{c}\left[3\beta\left(G'\right)^2 + \beta\left(A\right)^2\right]}{2\left[45\alpha^2 + 7\beta\left(\alpha\right)^2\right]}$$

⟸ ROA

⟸ Raman

- circular intensity difference for DCP_I ROA in backscattering geometry

$$\Delta_I\left(180^\circ\right) \equiv \frac{\Delta I_I\left(180^\circ\right)}{I_I\left(180^\circ\right)} = \frac{I_R^R - I_L^L}{I_R^R + I_L^L} = \frac{\frac{48}{c}\left[3\beta\left(G'\right)^2 + \beta\left(A\right)^2\right]}{2\left[6\beta\left(\alpha\right)^2\right]}$$

⟸ ROA

⟸ Raman

In the FFR approximation, backscattering ICP and DCP_I modulation schemes yield the same expression for ROA intensity, as has been demonstrated experimentally, but the corresponding Raman intensity is greater for the ICP experiment (polarized) than for the DCP_I one (depolarized).

Raman optical activity

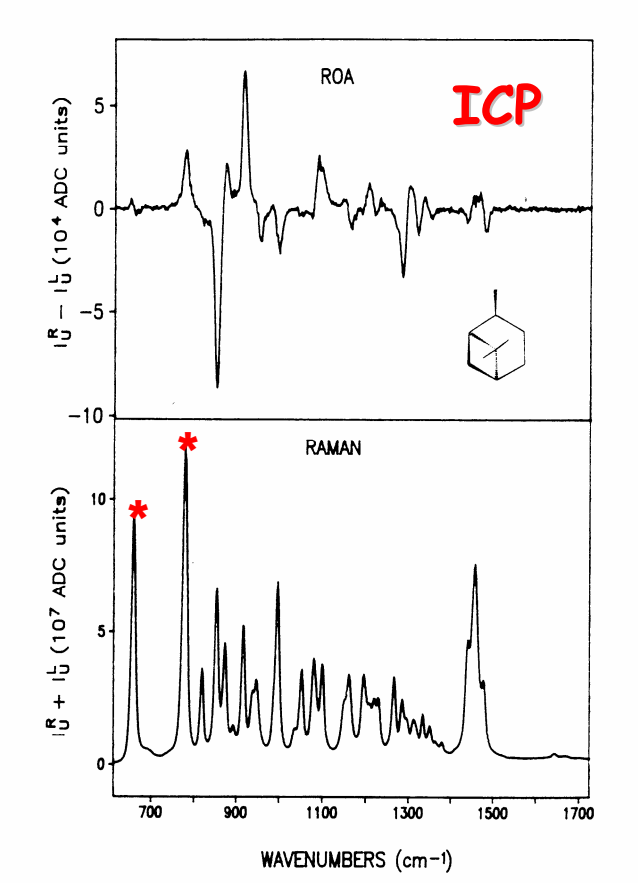

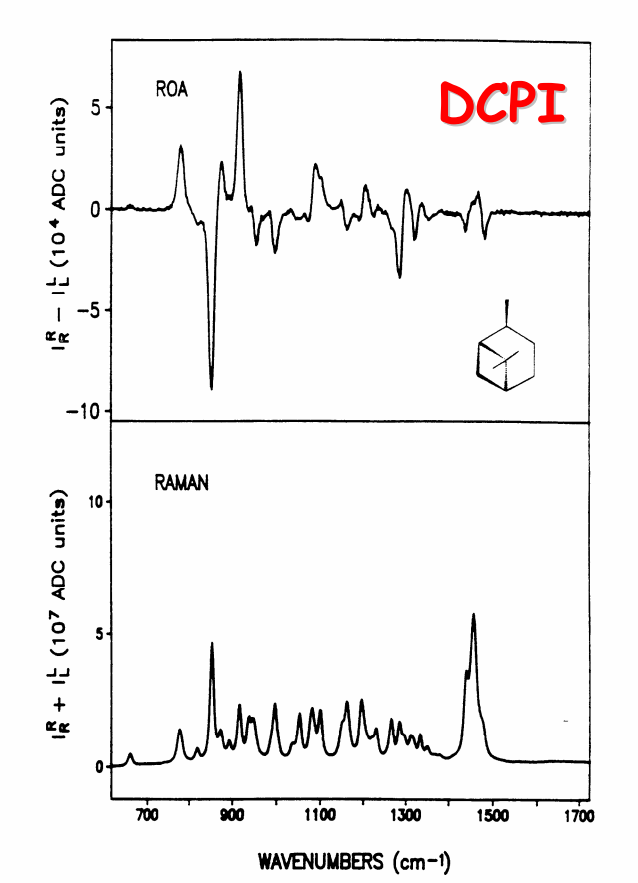

Comparison of ICP (left) and DCP_I (right) ROA and Raman spectra of (-)-*trans* pinane in backscattering geometry.

Raman optical activity – basic applications

- probe of absolute configuration, determination of stereo-conformational features of chiral molecules (in solution !!!)
- diagnostic tool to monitor optical purity (direct measurement of enantiomeric access) or identify chiral compounds from a chromatographic column
- structure elucidation of biologically significant molecules in solution including peptides, proteins, nucleic acids, carbohydrates, viruses, natural products, pharmaceutical molecules …)

Simulations of ROA spectra

(1S)-(-)-α-pinene

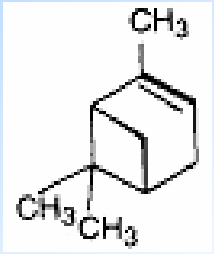

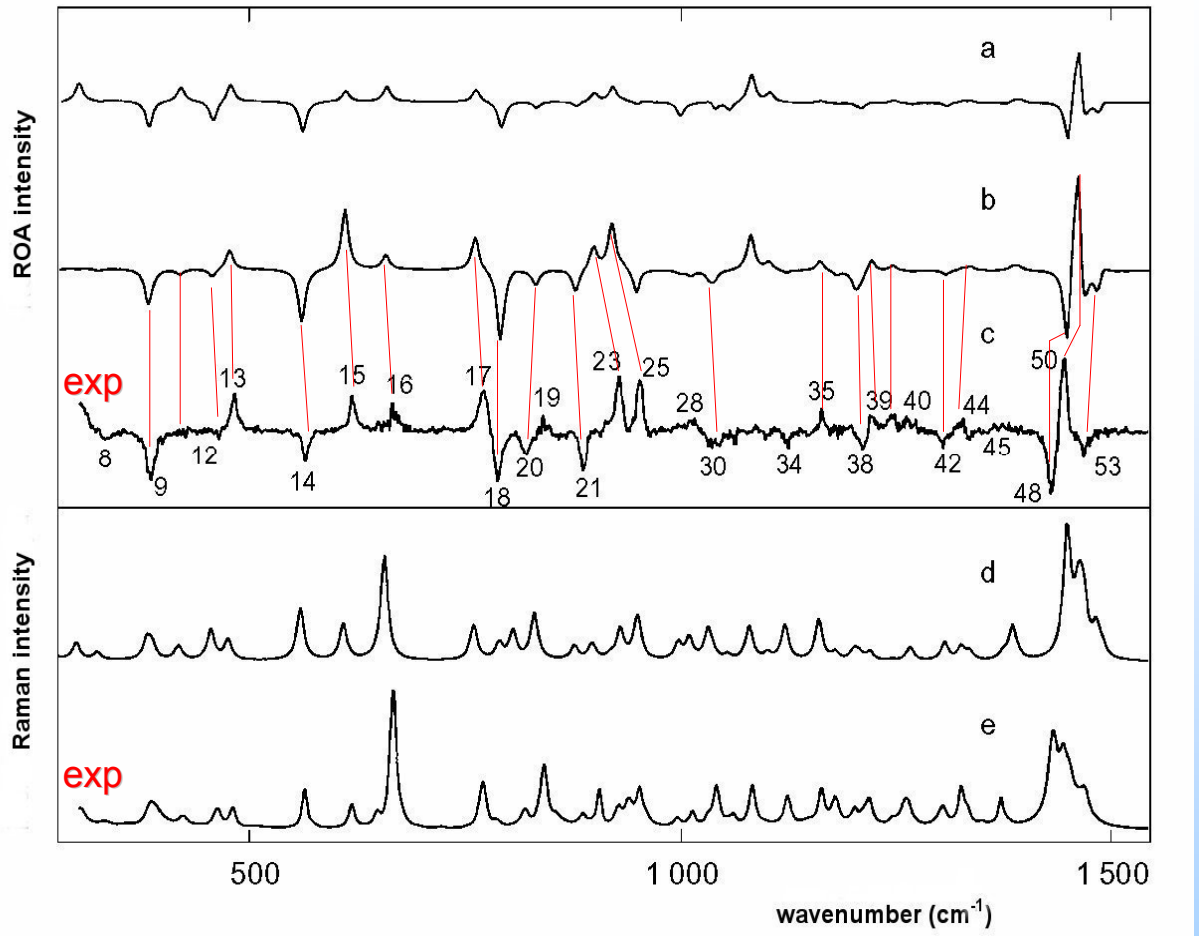

ROA and Raman spectra of (1S)-(-)-α-pinene: (a) simple (so called polar model) and (b) conventional model of ROA intensity calculation, (c) experimental ROA spectrum, (d) simulated and (e) experimental parent Raman spectrum.

Bouř et al., CCCC 62 (1997) 1384

Interpretation of ROA spectra

Several levels of interpretation:

- **Empirical** – identification of characteristic markers

Proteins

- **protein backbone vibrations**

  (C_α-C, C_α-C_β, C_α-N stretching)

  ~ 870 – 1150 cm^{-1}

- **extended amide III region**

  (N-H bending, C_α-N stretching + C_α-H bending)

  ~ 1230 – 1340 cm^{-1}

- **amide I** (*C=O stretching*)

  ~ 1630 – 1700 cm^{-1}

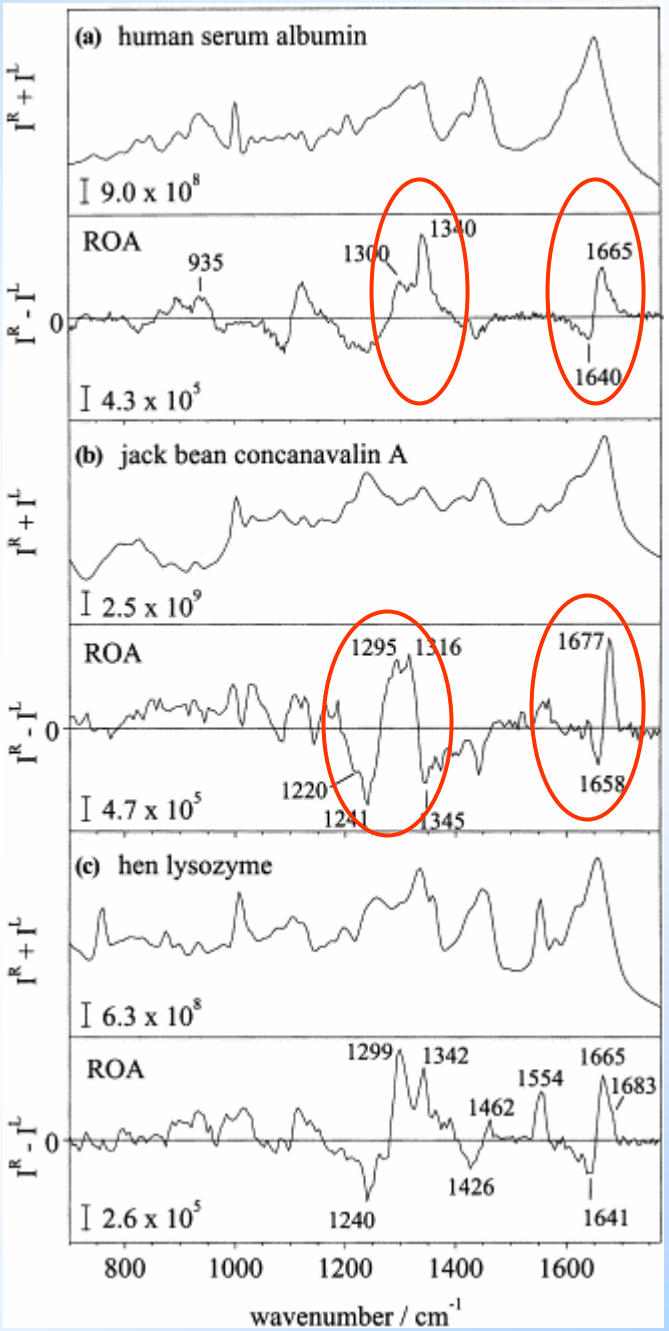

X-Ray PDB:

69,2% α-helix

1,7% 3_{10}-helix

43,5% β-sheet

1,7% α-helix

1.3% 3_{10}-helix

28,7% α-helix

10,9% 3_{10}-helix

6,2% β-sheet

Blanch et al., Vib. Spectrosc. 35 (2004) 87

Interpretation of ROA spectra

Several levels of interpretation:

- **Empirical** – identification of characteristic markers
- **Statistical methods** – e.g. principal component analysis

Proteins – Principal Component Analysis

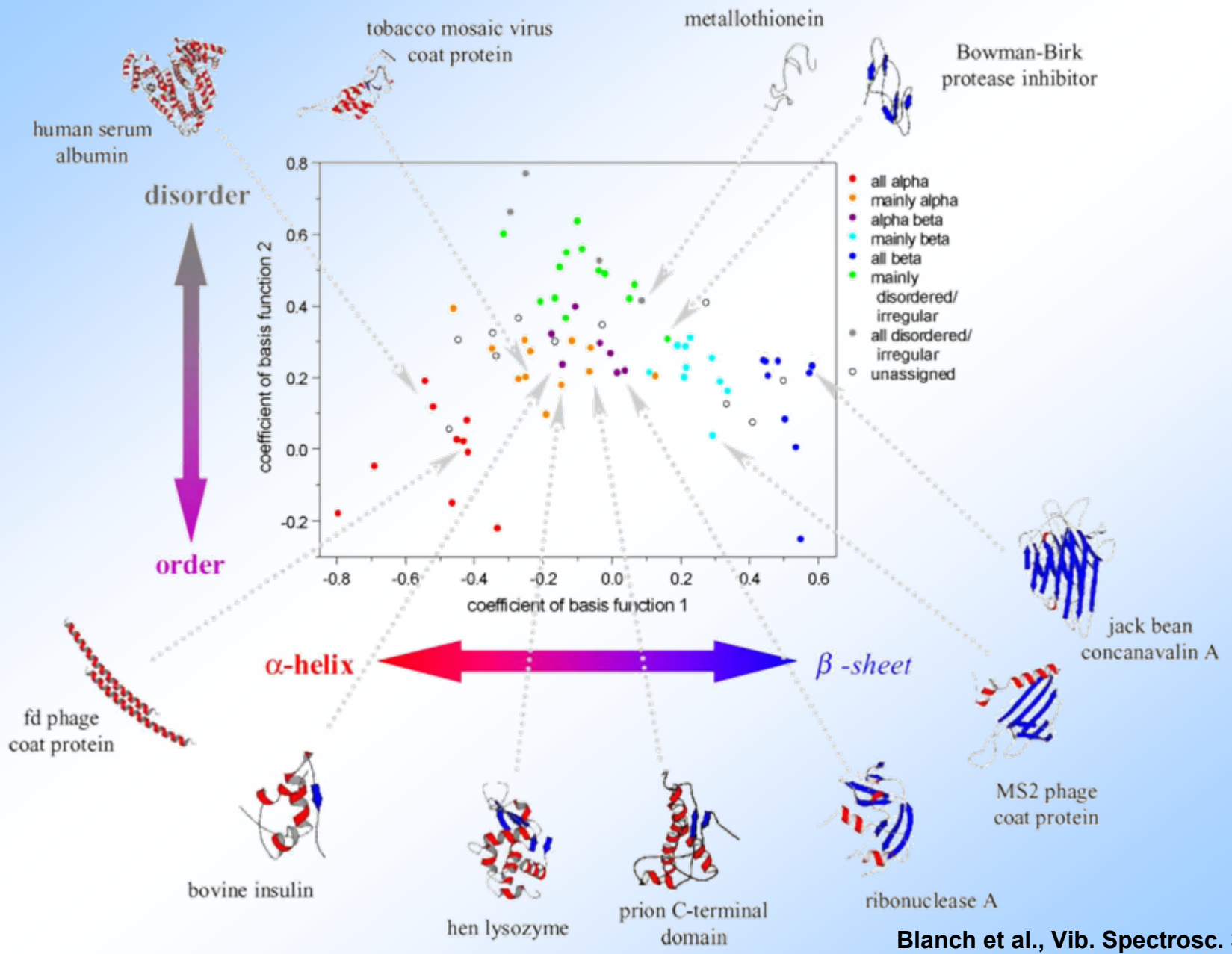

Blanch et al., Vib. Spectrosc. 35 (2004) 87

Interpretation of ROA spectra

Several levels of interpretation:

- **Empirical** – identification of characteristic markers
- **Statistical methods** – e.g. principal component analysis

Large biomolecules

GAP

- ***Ab initio* methods** (HF, DFT)

Small model systems

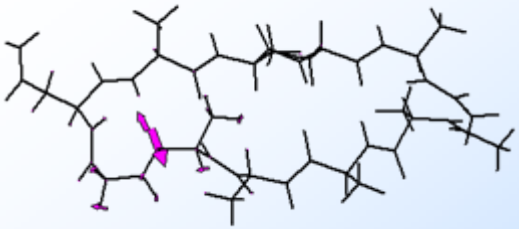

Ab initio calculations

Major limitations:

- **size** of studied systems
- interaction with **solvent** (zwittterionic molecules)
- system **flexibility** (real system x model)

Ab initio calculations – Overview

Conformer selection

Geometry Optimisation

- in **internal coordinates** (standard procedure)
- in **normal modes**[1] (useful for flexible molecules or clusters with water; normal modes with energies lower than a treshold can be constrained)
- methods involving **electron correlation** (**DFT**, MP2)

Frequencies

- same level as above (COSMO/B3LYP/6-31**++**G******)

Intensities

- derivatives of **polarizability** and **optical activity tensors**) computationally very demanding (vacuum/HF/6-31G)

Comparison with Experiment

[1]**Bouř et al., J. Chem. Phys. 117 (2002) 4126**

Solvent simulations

Implicit solvent models

- **Onsager** dipole model (the simplest)

spherical cavity in dielectrics

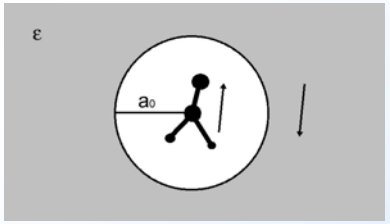

- ***COSMO*** (*CO*nductor like *S*creening *MO*del) more flexible and more realistic

COSMO cavity around proline molecule; colors correspond to charge induced on the surface by the molecule

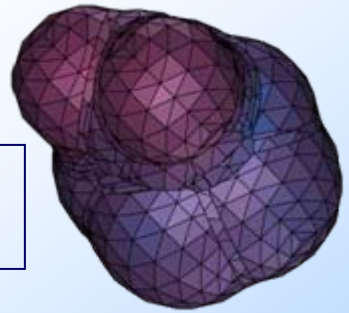

Explicit solvent models

- solvation with explicit molecules of water

4 conformations of proline calculated with explicit water molecules

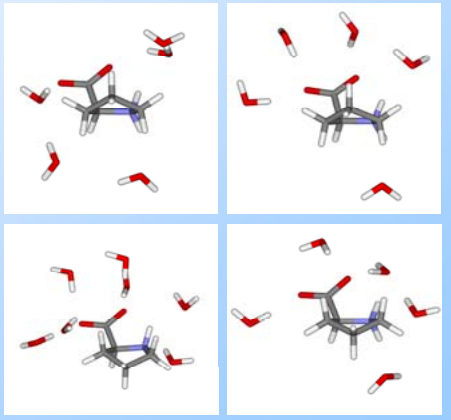

L-Alanine

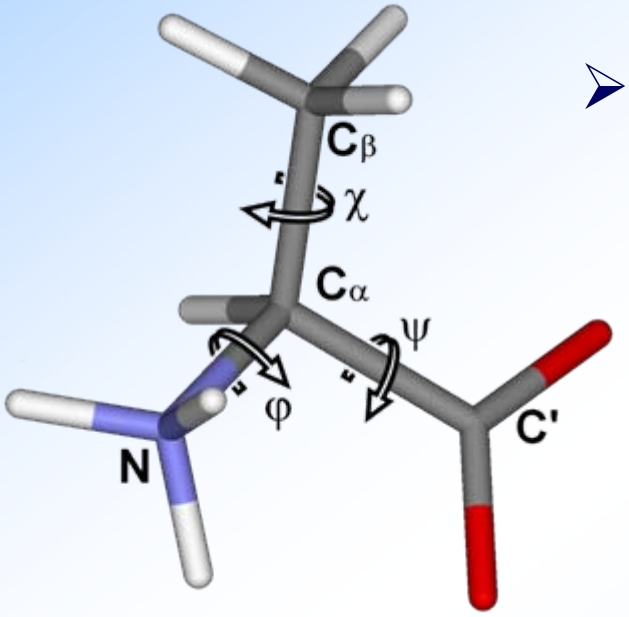

- the simplest amino acid
- ideal benchmark system for studying:
  - conformational behavior
  - interaction with solvent

L-Alanine – potential energy surface

1D scan

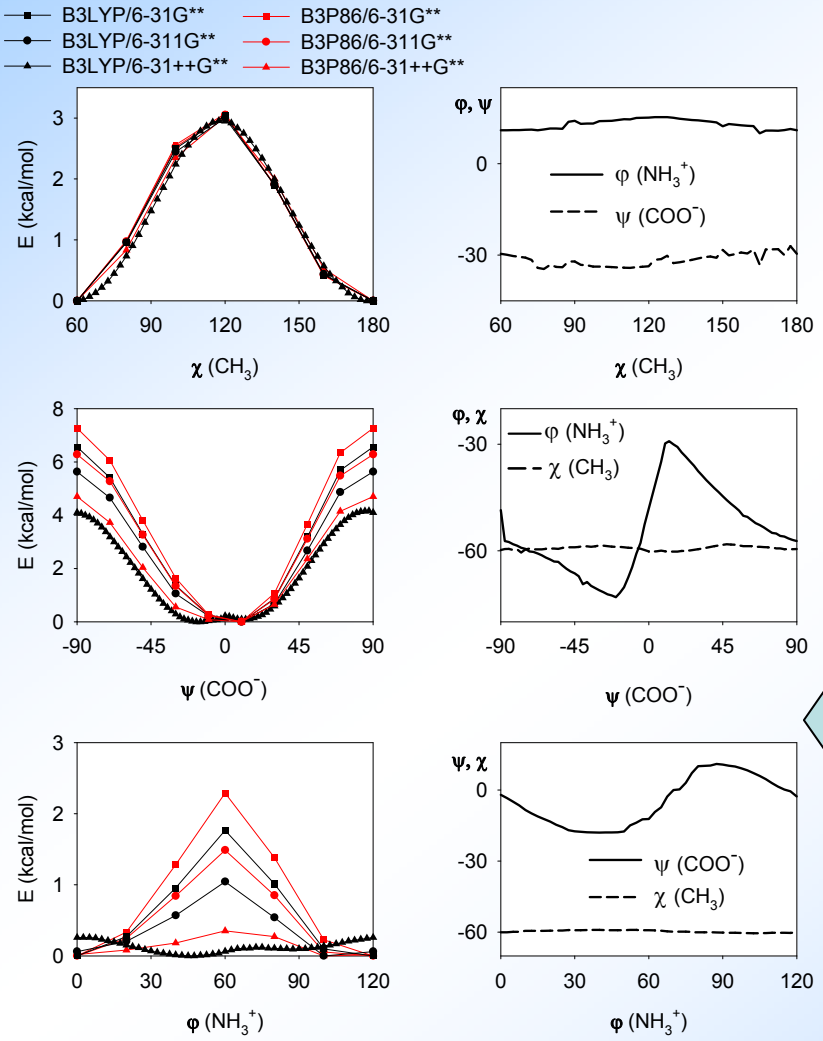

2D scan

B3LYP/COSMO/6-31++G**

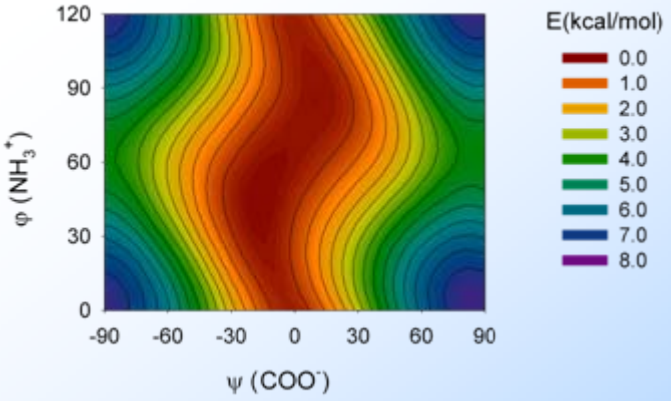

Dependencies of molecular energy (E, left) and dihedral angles (right) on the angles φ, ψ, and χ. The remaining coordinates in the one-dimensional scans were allowed to fully relax.

Kapitán et al., J. Phys. Chem. 110 (2006) 4689

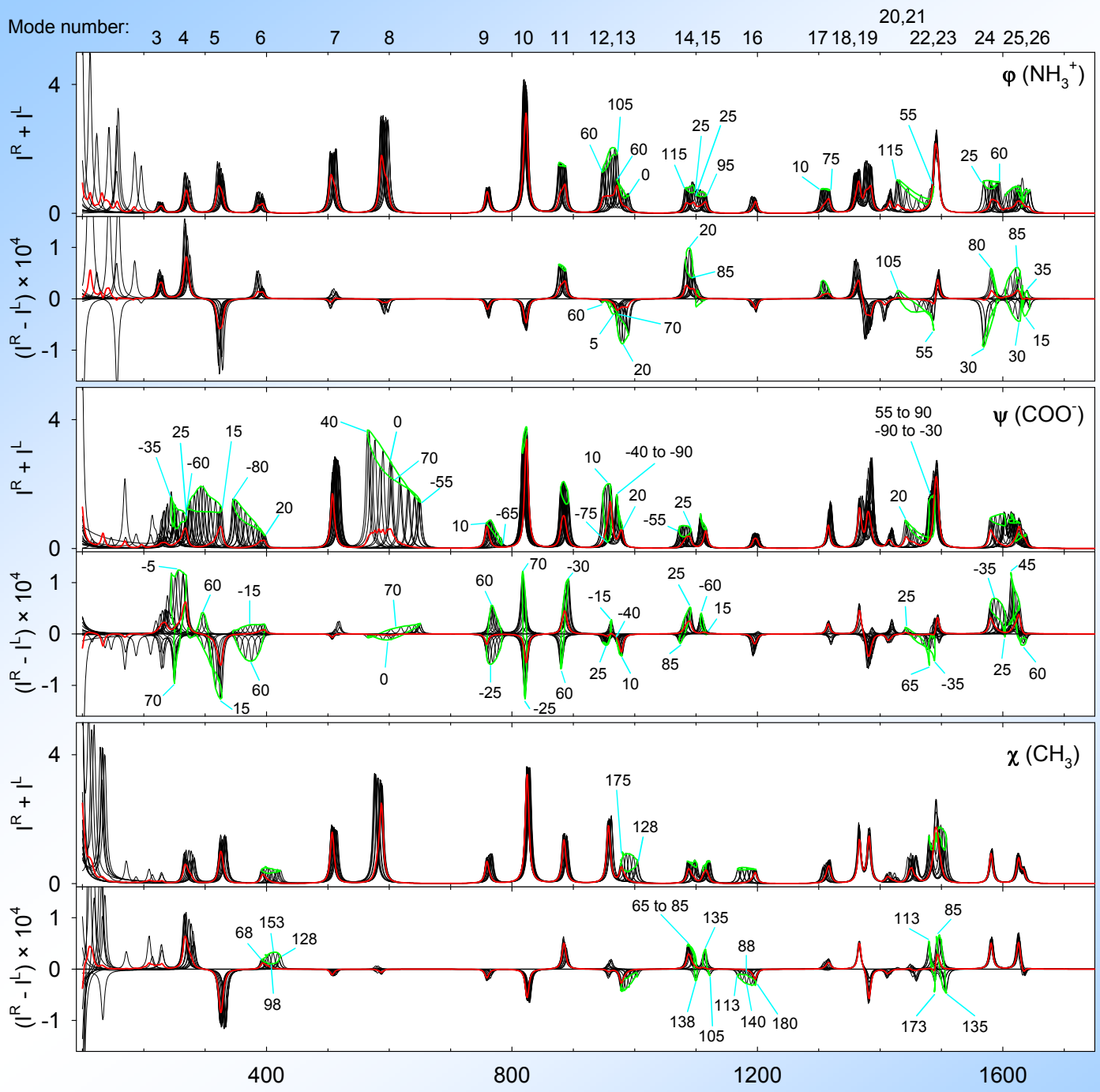

NH_3^+

COO^-

CH_3

Kapitán et al., J. Phys. Chem. 110 (2006) 4689

L-Alanine

- Raman and ROA spectra can be reliably interpreted if the movement of flexible molecular parts is considered

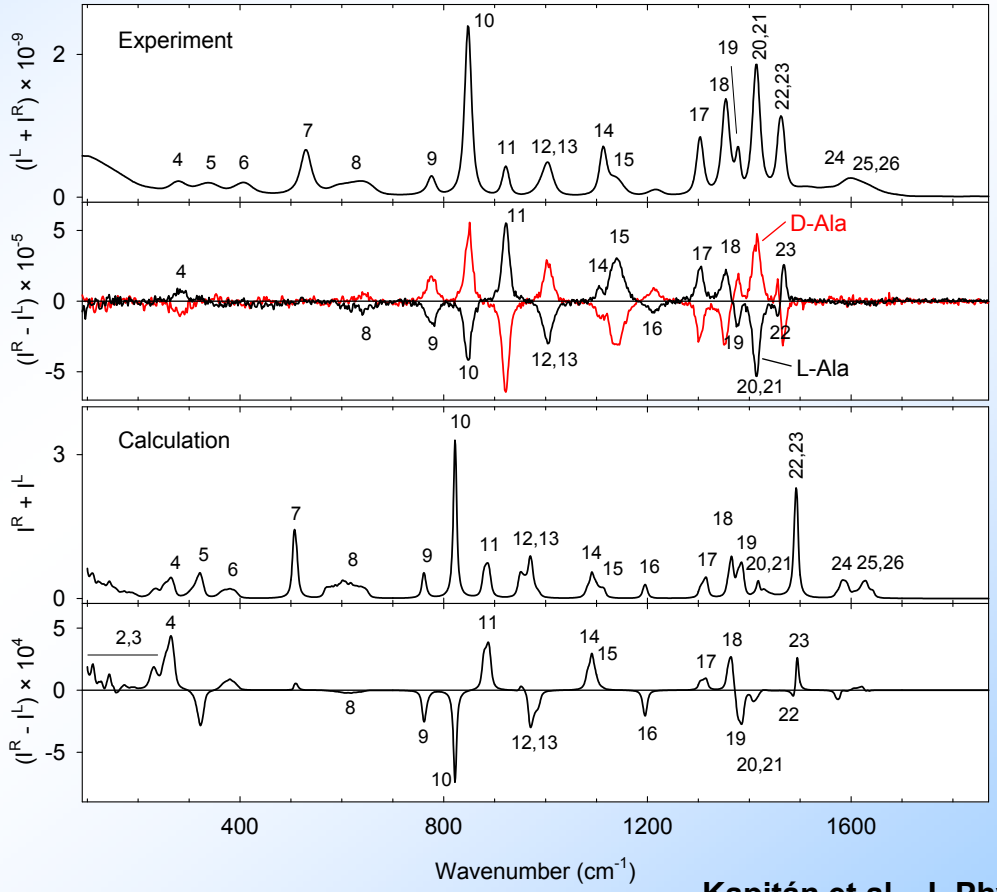

Raman

ROA

Kapitán et al., J. Phys. Chem. 110 (2006) 4689

L-Proline

- proline exhibits two major conformations with very similar energies ($\Delta E < 0.3$ kcal/mol)

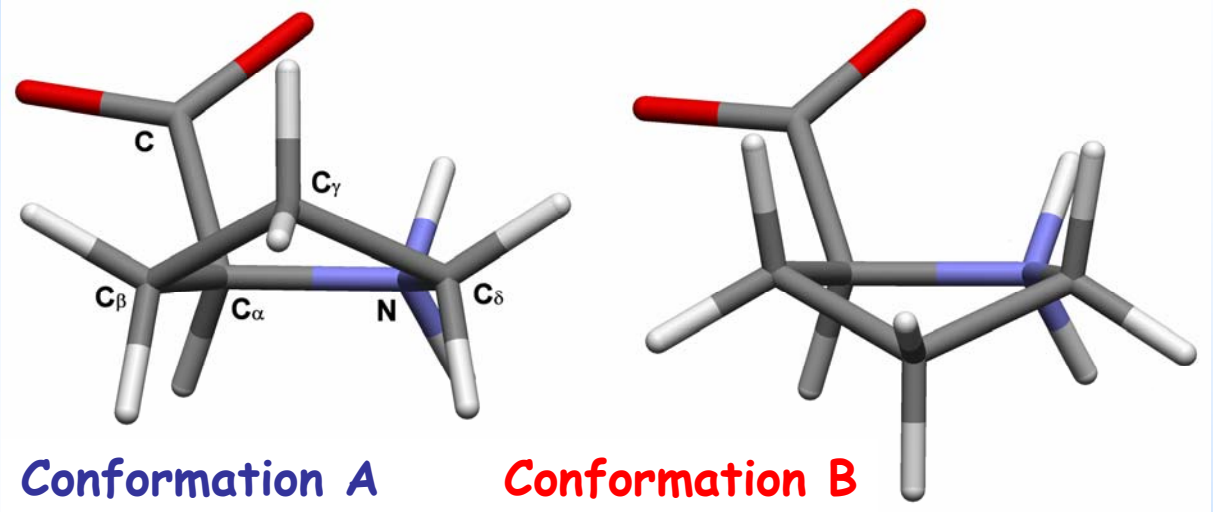

- conformational space of proline was investigated in detail by **rotating the COO^- group** and **ring puckering**
- checked influence of water molecules

L-Proline – ring puckering

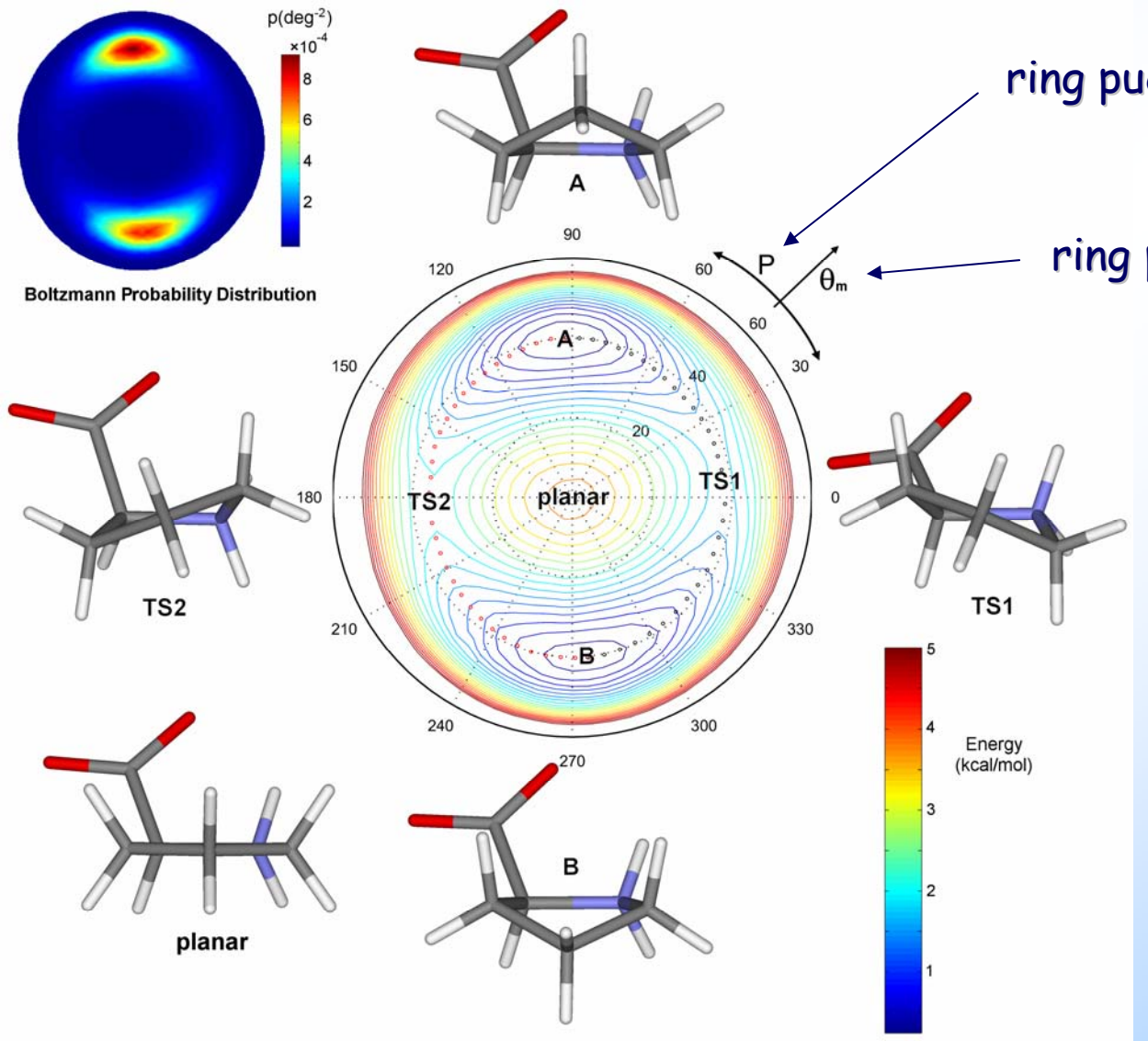

ring puckering phase[1]

ring puckering amplitude[1]

[1]Altona et al., JACS 94 (1972) 8205

Dependent rotation of COO^- group:

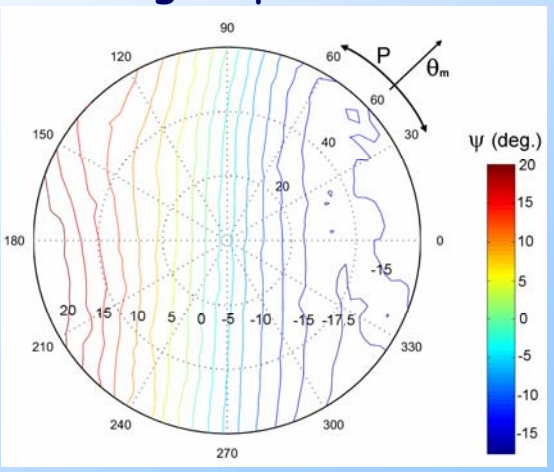

L-Proline – rotation of COO^- group

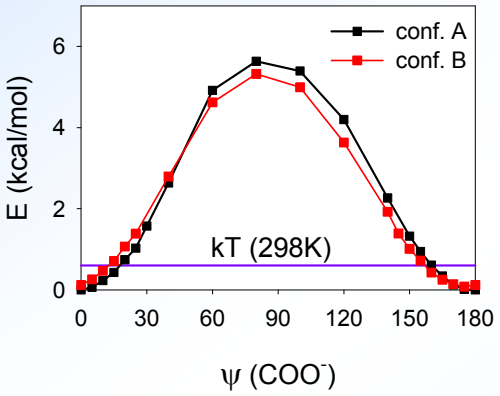

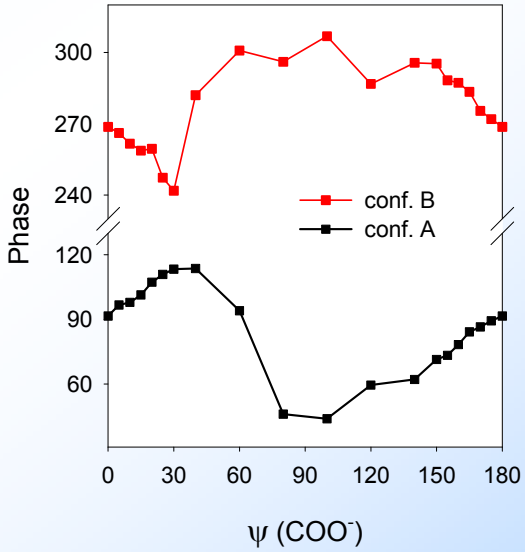

L-Proline – different approaches

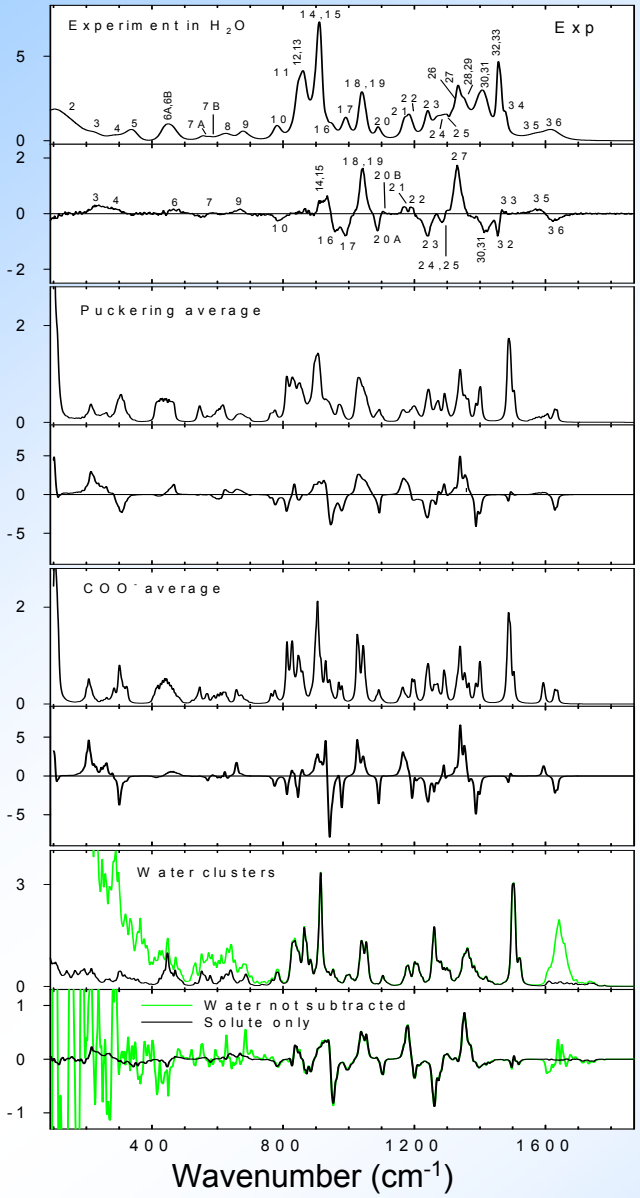

Experiment

Ring puckering

Rot. COO^-

Water clusters

Model dipeptides

There is a significant difference between

Ala-Pro x Pro-Ala

Gly-Pro x Pro-Gly

ROA (Raman) can directly reflect flexibility of the molecule

Model dipeptides

rigidity × *flexibility*

Gly-Pro

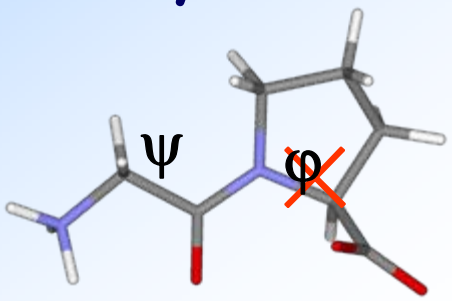

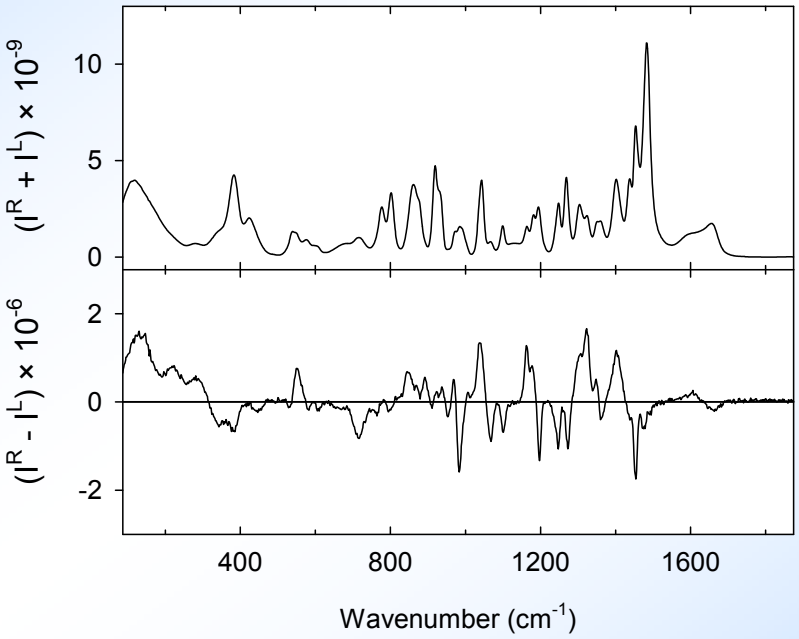

Pro-Gly

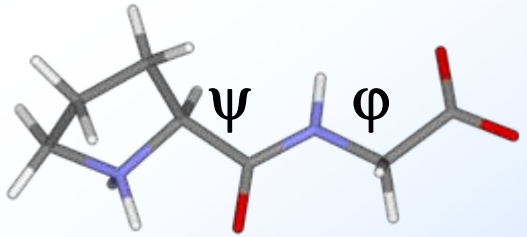

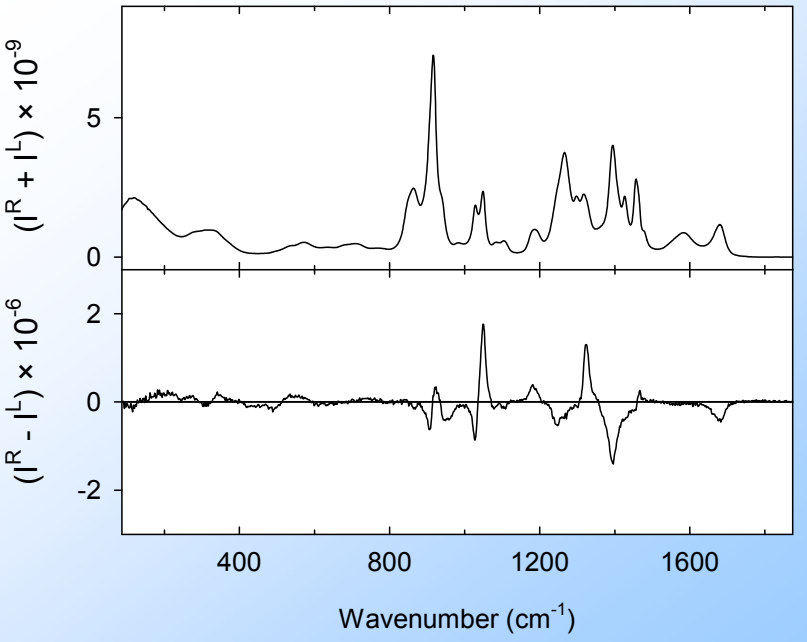

Poly(L-Proline)

- in **polyproline II** (PPII) conformation (ϕ=-78°, ψ=149°) left-handed 3_1-helix

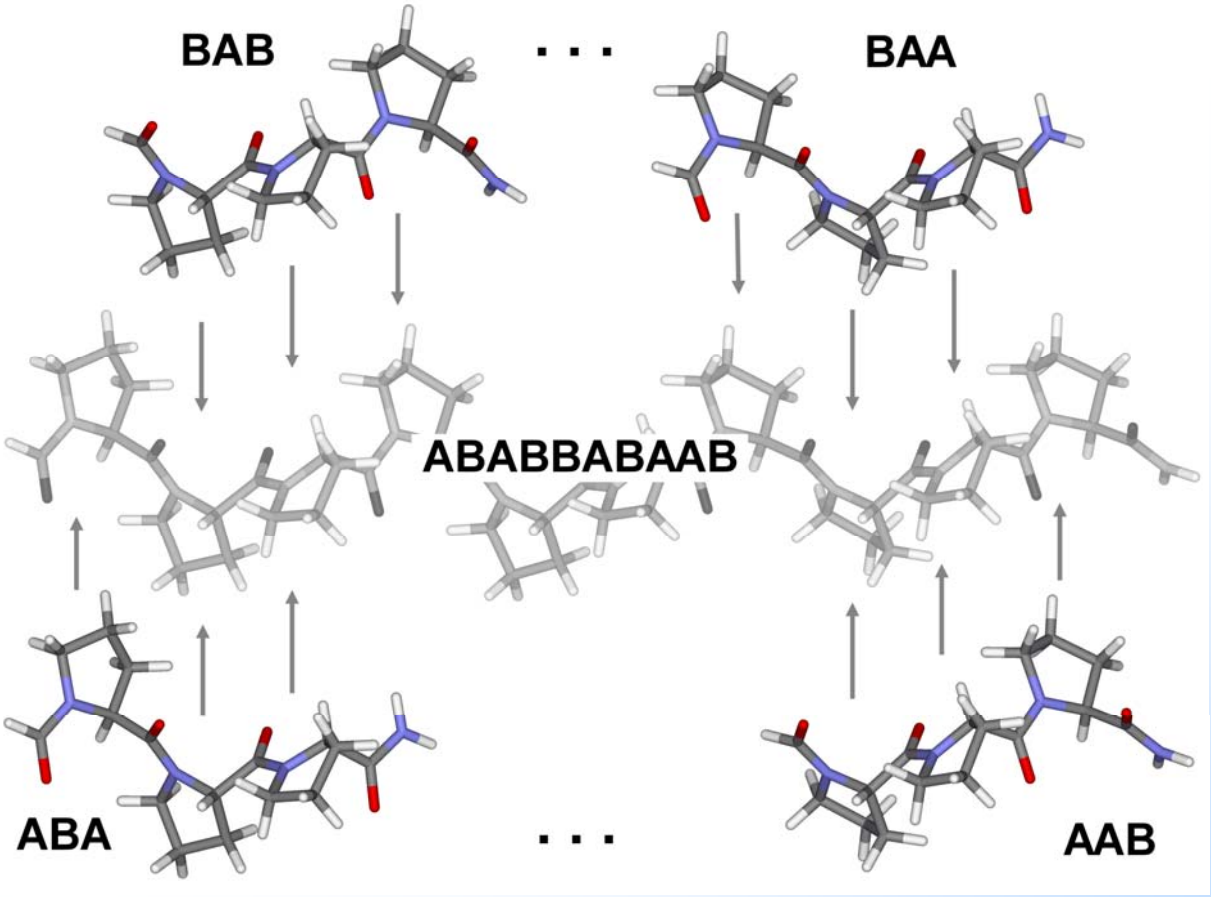

Schematic representation of the tensor transfer technique.

Atomic property tensors in the tripeptides were obtained *ab initio* and transferred by propagation of these smaller fragments along the longer polypeptide chain.

Poly(L-Proline) – ring conformation

- generated 20-mer sequences with different A/B conformational content
- averaging over 50 generated sequences

A  B

Raman

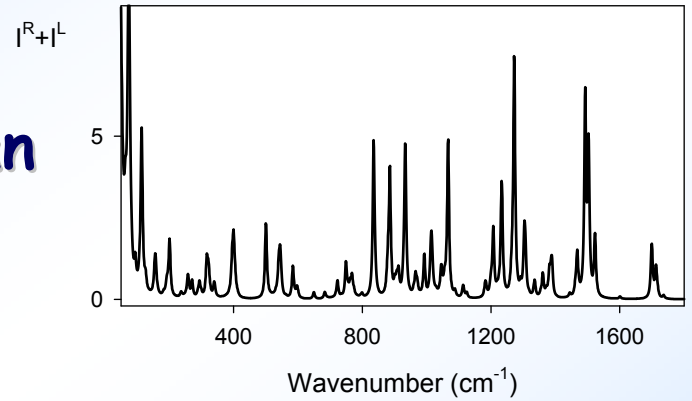

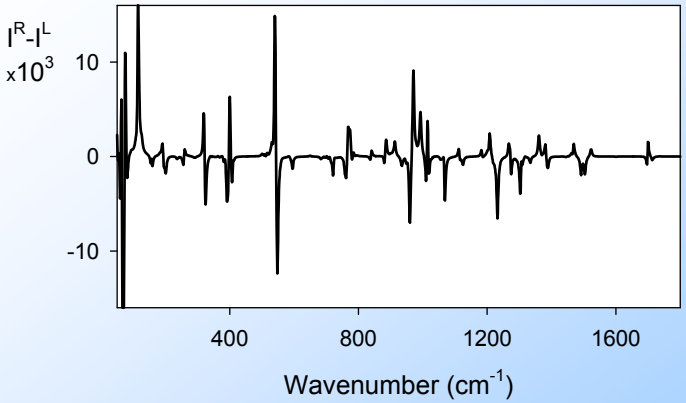

ROA

Poly(L-Proline) – ring conformation

- generated 20-mer sequences with different A/B conformational content
- averaging over 50 generated sequences

Raman

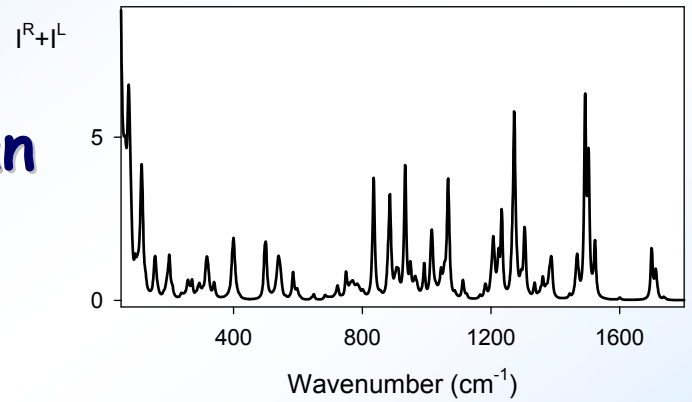

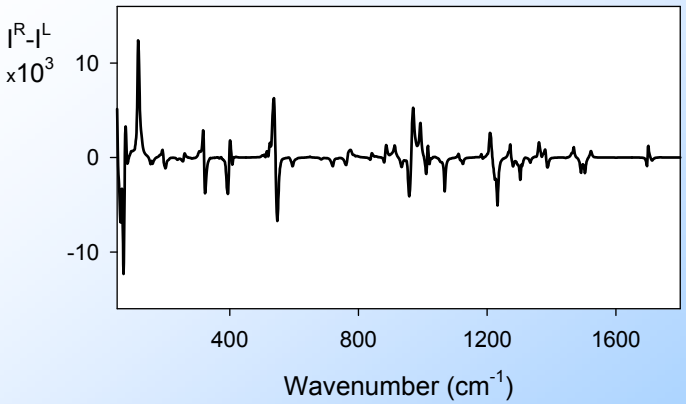

ROA

Poly(L-Proline) – ring conformation

- generated 20-mer sequences with different A/B conformational content
- averaging over 50 generated sequences

Raman

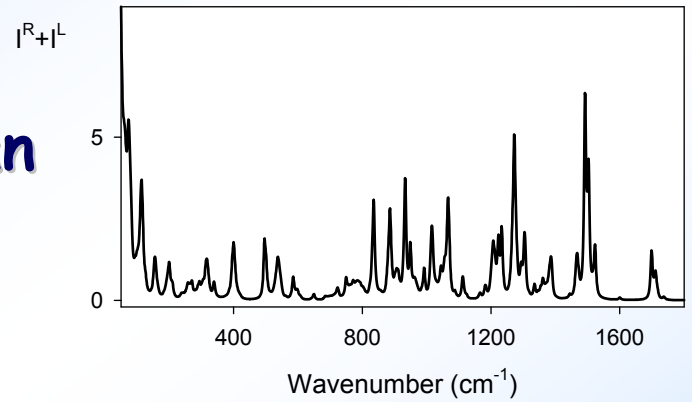

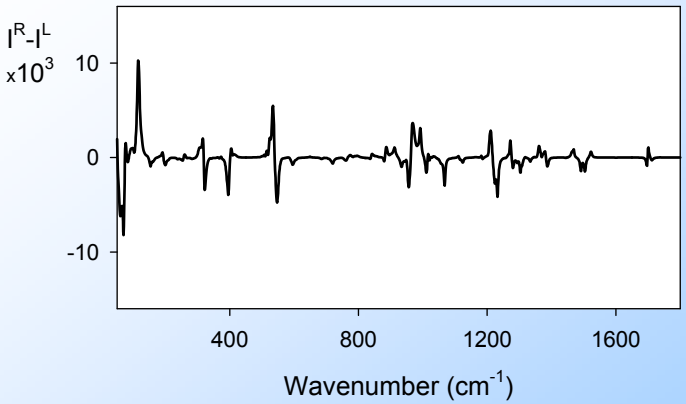

ROA

Poly(L-Proline) – ring conformation

- generated 20-mer sequences with different A/B conformational content
- averaging over 50 generated sequences

Raman

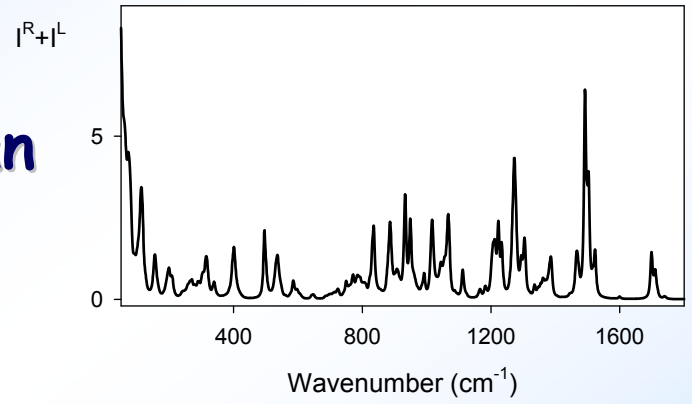

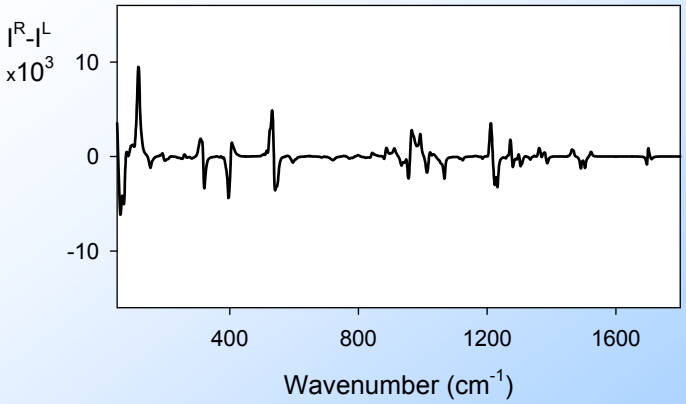

ROA

Poly(L-Proline) – ring conformation

- generated 20-mer sequences with different A/B conformational content
- averaging over 50 generated sequences

Raman

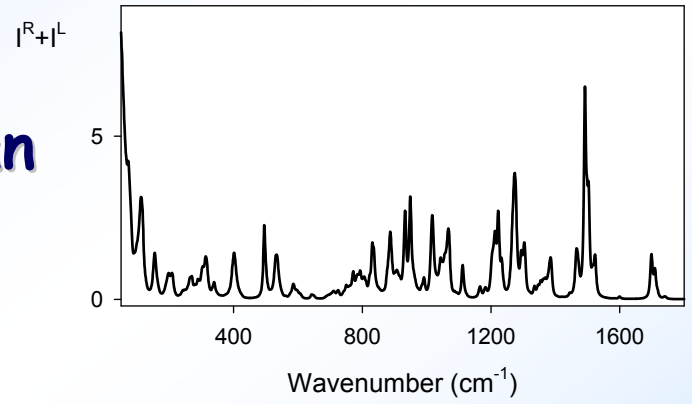

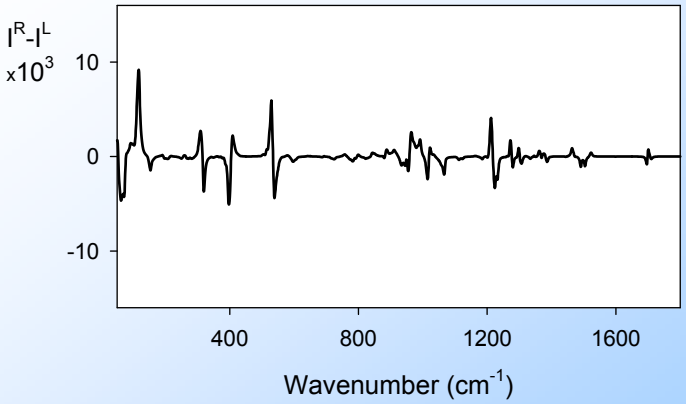

ROA

Poly(L-Proline) – ring conformation

- generated 20-mer sequences with different A/B conformational content
- averaging over 50 generated sequences

Raman

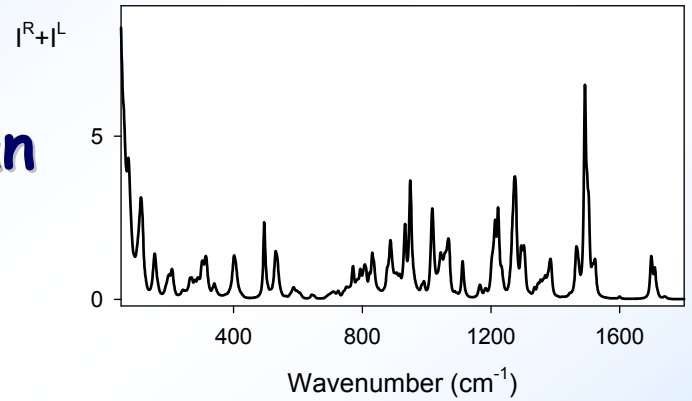

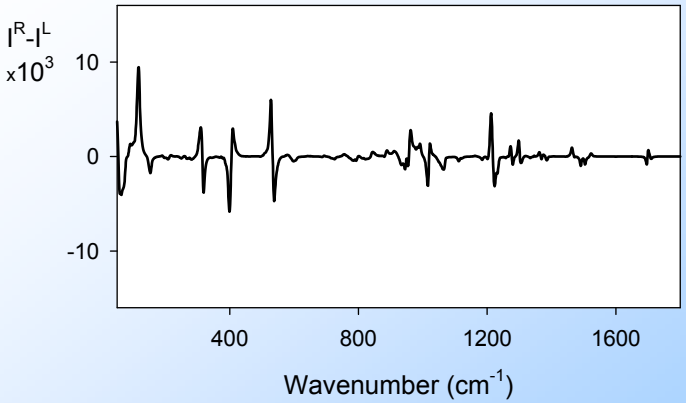

ROA

Poly(L-Proline) – ring conformation

- generated 20-mer sequences with different A/B conformational content
- averaging over 50 generated sequences

Raman

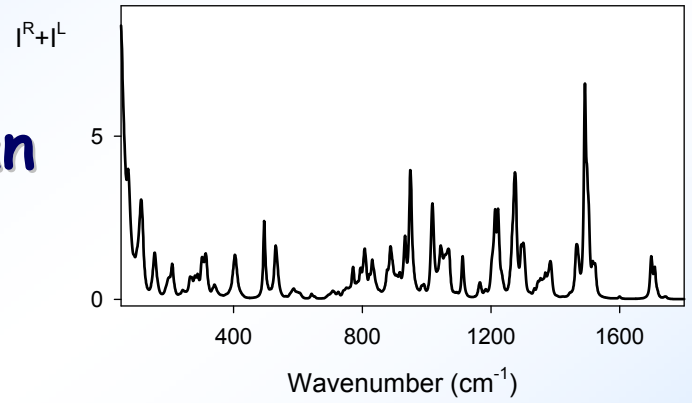

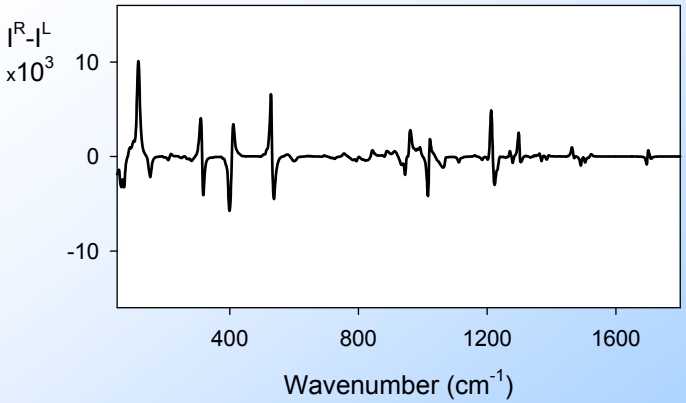

ROA

Poly(L-Proline) – ring conformation

- generated 20-mer sequences with different A/B conformational content
- averaging over 50 generated sequences

Raman

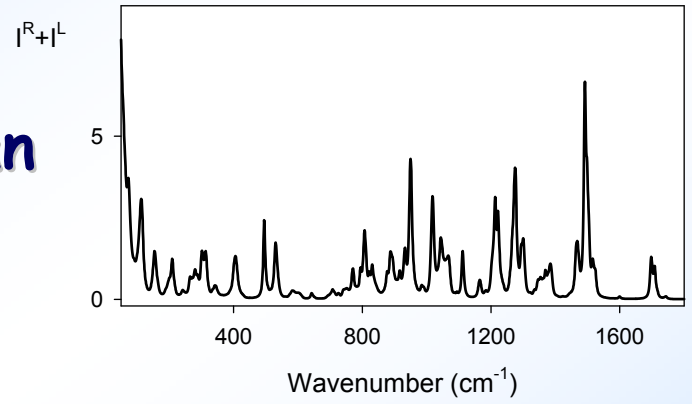

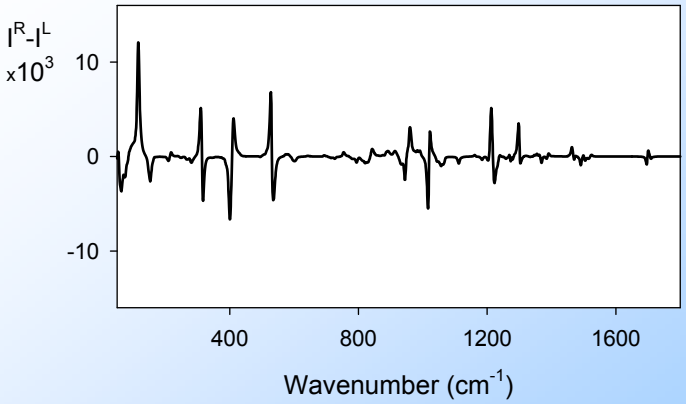

ROA

Poly(L-Proline) – ring conformation

- generated 20-mer sequences with different A/B conformational content
- averaging over 50 generated sequences

Raman

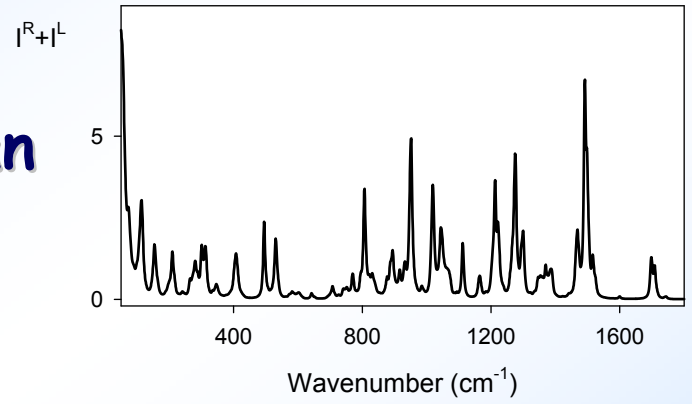

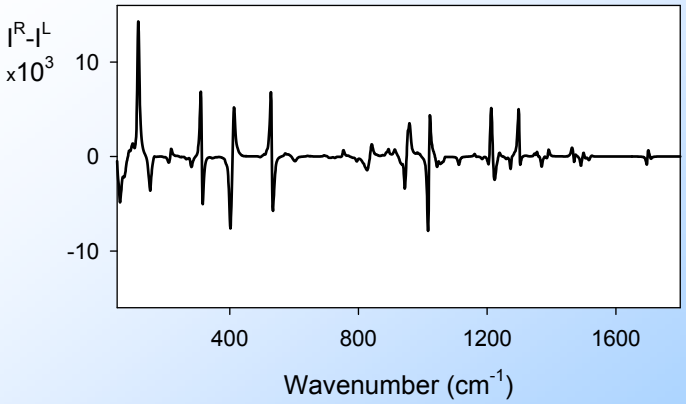

ROA

Poly(L-Proline) – ring conformation

- generated 20-mer sequences with different A/B conformational content
- averaging over 50 generated sequences

Raman

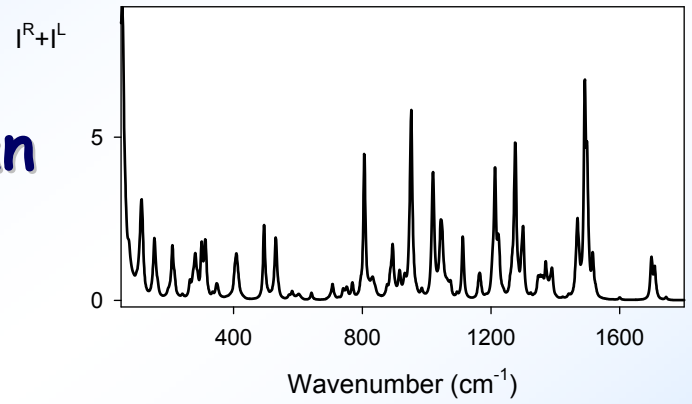

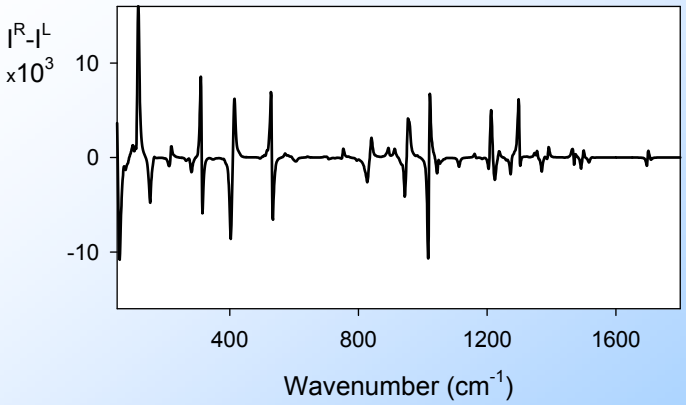

ROA

Poly(L-Proline) – ring conformation

- generated 20-mer sequences with different A/B conformational content
- averaging over 50 generated sequences

A B

Raman

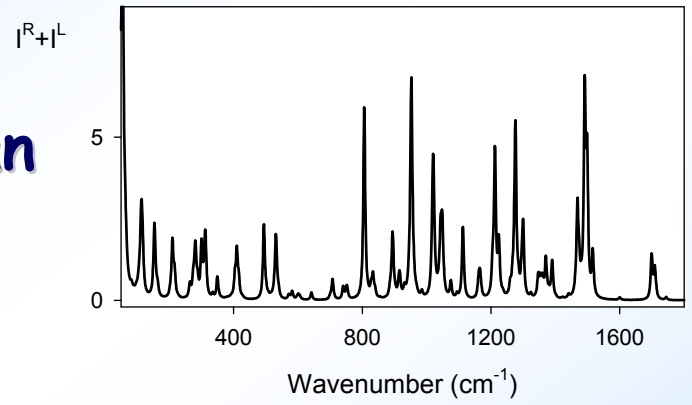

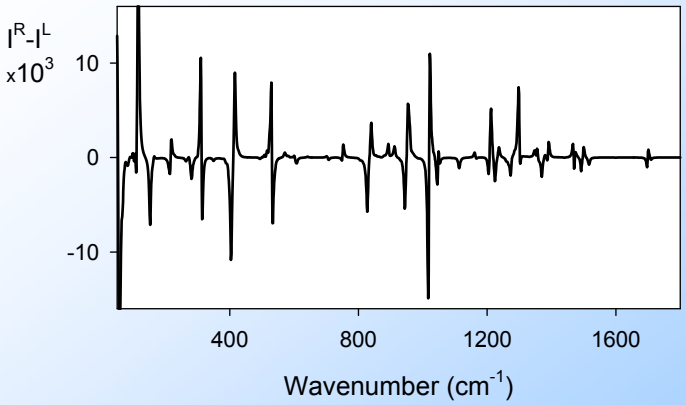

ROA

Poly(L-Proline) – grand finale

- Comparison of experimental data with simulated 20-mer A:B=1:1

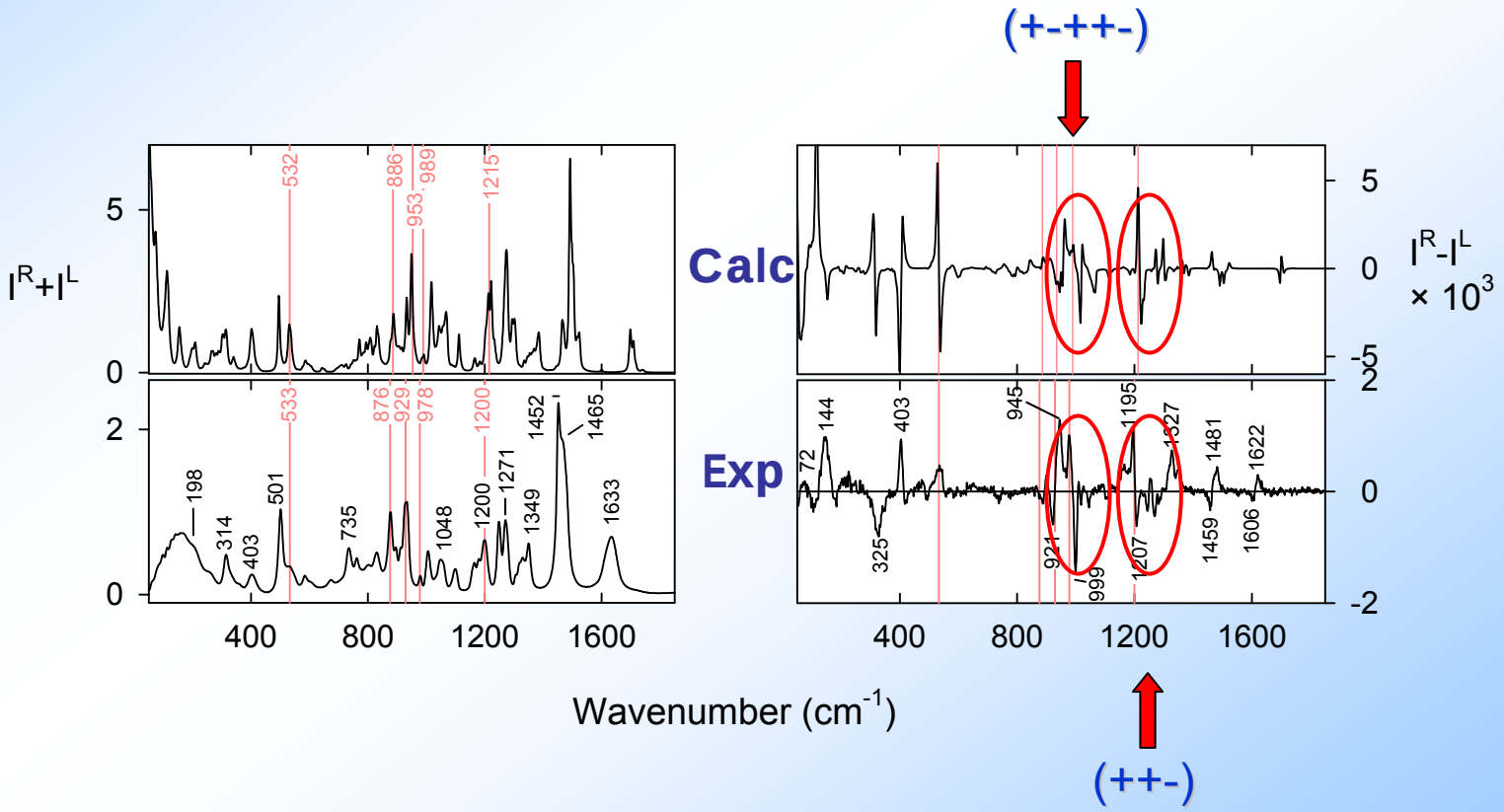

Kapitán et al., JACS 128 (2006) 2438

Hinge peptide and its analogs

HINGE peptide is a fragment 225-232/225'-232' from the core of human immunoglobulin IgG1. It acts in this parent molecule as a swivel point crosslinking two rather heavy peptide chains. Being a parallel dimer of the octapeptide H-Thr-Cys-Pro-Pro-Cys-Pro-Ala-Pro-OH (C_2 symmetry). The sequence is rich in proline residues and is expected to be quite rigid also due to a presence of two disulphide bridges. The peptide offers several advantages for use as a universal carrier of various active sequences (immunologically neutral, possesses six independent terminal groups: -NH and -OH on Thr residues and C-terminal carboxyl).

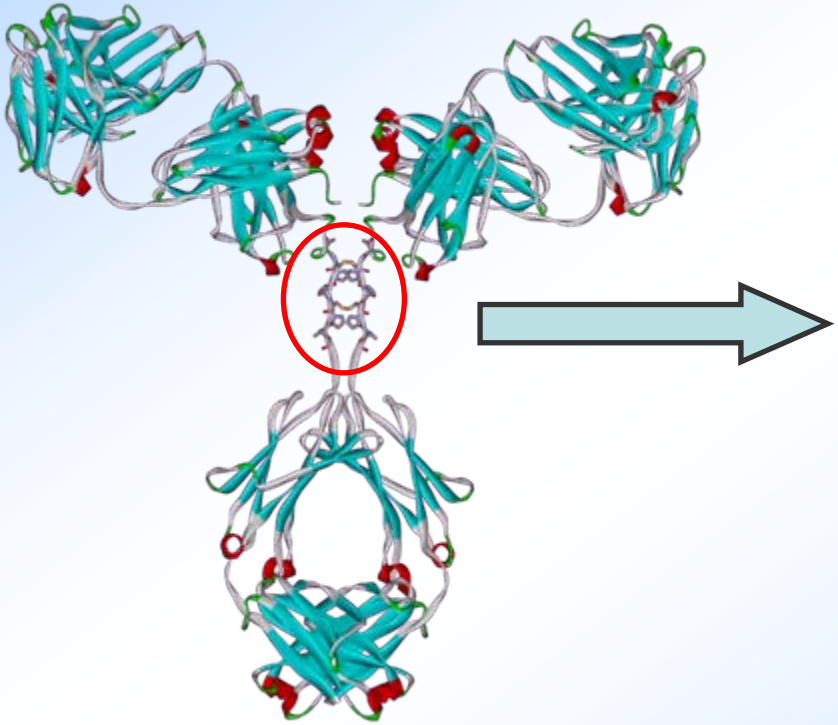

▲ Model of an entire human IgG1 molecule.[1]

hinge peptide (double thread)

single thread Met analog

S-S bridged tetrapeptide $(H\text{-Gly-Cys-OH})_2$

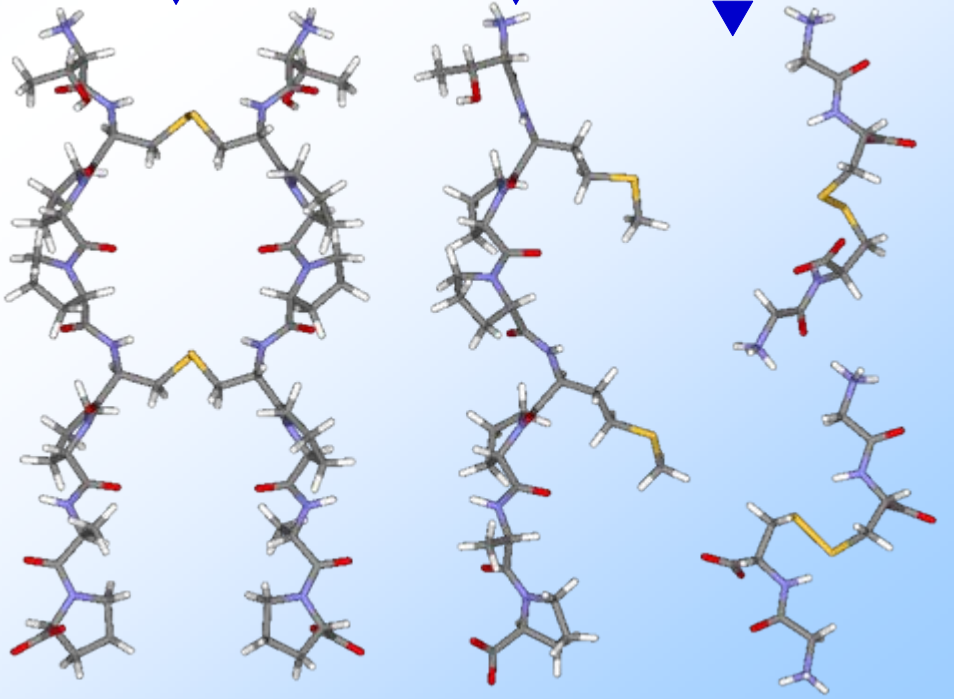

[1]Padlan E.A, *Mol. Immunol.* **31** (1994) 169.

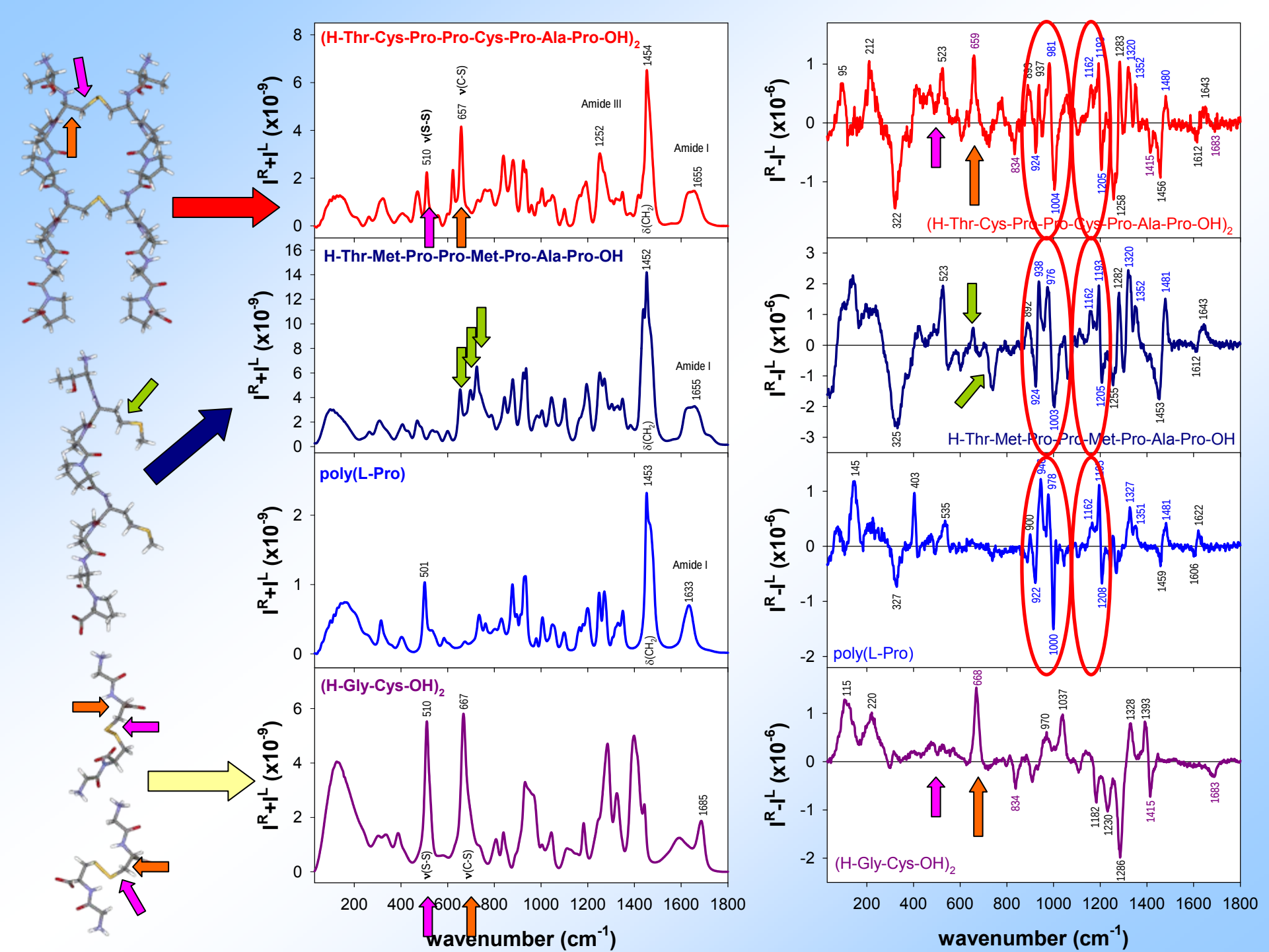
(H-Thr-Cys-Pro-Pro-Cys-Pro-Ala-Pro-OH)2
H-Thr-Met-Pro-Pro-Met-Pro-Ala-Pro-OH
poly(L-Pro)
(H-Gly-Cys-OH)2
I^R+I^L (x10^-9)
I^R-I^L (x10^-6)
wavenumber (cm^-1)
ν(S-S)
ν(C-S)
Amide III
Amide I
δ(CH2)

Summary

- successful reconstruction of **ROA spectrometer**
- spectra of selected biomolecular systems were successfully measured and interpreted

  - **new approaches to simulation** of Raman and ROA spectra were developed
  - it is essential **to take into account dynamic factors** for successful simulation
  - **conformational flexibility** of molecules affect significantly Raman and ROA spectra and can offer good estimate of system rigidity or flexibility
  - previously neglected **low energy vibrations** (below 600 cm^{-1}) are very sensitive to conformational changes and can give new insight into molecular flexibility.

Acknowledgement

Josef Kapitán

Petr Bouř

Jiří Bok Petr Praus

Petr Maloň Jaroslav Šebestík
Hana Hulačová

GAČR, GAUK, MŠMT (výzkumný záměr)

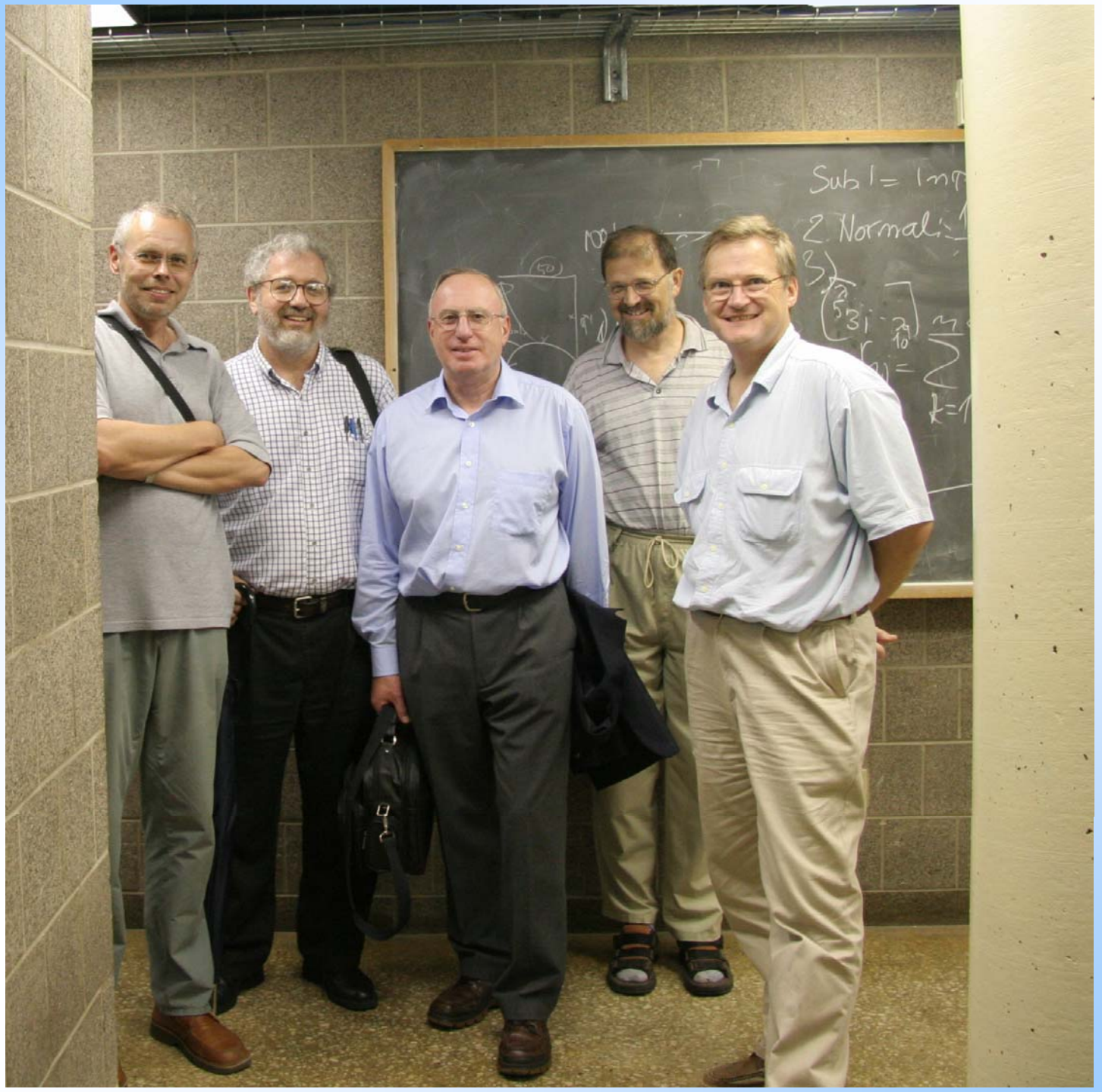
Sub 1 = Imp
2. Normal:
3.